

1

2

3

4

5 **Transfer RNA Genes Affect Chromosome Structure and Function via Local**
6 **Effects**

7 Omar Hamdani^{1*}, Namrita Dhillon^{1*}, Tsung-Han S. Hsieh^{3*}, Takahiro Fujita^{4*}, Josefina
8 Ocampo^{5*}, Jacob G. Kirkland¹, Josh Lawrimore⁶, Tetsuya J. Kobayashi⁷, Brandon
9 Friedman⁶, Derek Fulton⁶, Kenneth Y. Wu¹, Răzvan V. Chereji⁵, Masaya Oki⁴, Kerry
10 Bloom⁶, David J Clark⁵, Oliver J. Rando³, Rohinton T. Kamakaka^{1,2}

11

12

13

14

15 1 Department of MCD Biology, 1156 High Street, University of California, Santa
16 Cruz, CA 95064 USA

17 E-mail: rohinton@ucsc.edu

18 2 Corresponding Author

19 3 Department of Biochemistry and Molecular Pharmacology, University of
20 Massachusetts Medical School, Worcester, MA 01605, USA

21 4 Department of Applied Chemistry Biotechnology, University of Fukui, Bunkyo,
22 Fukui, Japan.

23 5 Division of Developmental Biology, Eunice Kennedy Shriver National Institute of
24 Child Health and Human Development, 6 Center Drive, Bethesda MD 20892 USA

25 6 Department of Biology, University of North Carolina at Chapel Hill, Chapel Hill,
26 NC 27599-3280 USA

27 7 Institute of Industrial Science, The University of Tokyo, Tokyo, Japan

28

29

30

31

* These authors contributed equally

32 **Abstract**

33 The genome is packaged and organized in an ordered, non-random manner and
34 specific chromatin segments contact nuclear substructures to mediate this organization.
35 Transfer RNA genes (tDNAs) are binding sites for transcription factors and architectural
36 proteins and are thought to play an important role in the organization of the genome. In
37 this study, we investigate the role of tDNAs in genomic organization and chromosome
38 function by editing a chromosome so that it lacks any tDNAs. Surprisingly our analyses
39 of this tDNA-less chromosome show that loss of tDNAs does not grossly affect
40 chromatin architecture or chromosome tethering and mobility. However, loss of tDNAs
41 affects local nucleosome positioning and the binding of SMC proteins at these loci. The
42 absence of tDNAs also leads to changes in centromere clustering and a reduction in the
43 frequency of long-range *HML-HMR* heterochromatin clustering with concomitant effects
44 on gene silencing. We propose that the tDNAs primarily affect local chromatin structure
45 that result in effects on long-range chromosome architecture.

46

47 **Introduction**

48 The three dimensional organization of the yeast nucleus is non-random (Reviewed
49 in [1, 2]). Each chromosome occupies a specific territory in the nucleus anchored to
50 nuclear substructures via specific DNA sequences. The telomeres of each chromosome
51 tend to associate with one another and with the nuclear envelope in small clusters,
52 based on the length of the chromosome arms [3-5]. The rDNA repeats on chromosome
53 XII are packaged into a dense structure known as the nucleolus, which also localizes to
54 the nuclear periphery [6]. Opposite the nucleolus is the spindle pole body, which is the
55 interphase attachment site for the centromeres of the 16 chromosomes [7]. Attachment
56 of centromeres to the spindle pole and attachment of telomeres to the nuclear
57 membrane dependent upon chromosome arm length helps organize the nucleus [8].
58 The active genes along the chromosome arms primarily reside in the nuclear interior
59 though some active genes including some tRNA genes interact with nuclear pores and
60 help tether the arms [1, 9, 10].

61 Besides DNA sequence elements, numerous proteins play a role in nuclear
62 organization via networks of interactions between nuclear membrane and chromatin
63 bound proteins. Chromatin bound proteins involved in this organization include
64 heterochromatin proteins, [11], lamin like proteins [12-16], specific transcription factors
65 [17, 18], RNA polymerases [6] and DNA repair proteins [19, 20] (see [1] for review).

66 tRNA genes (tDNAs) are a class of active genes found on all chromosomes and are
67 bound by transcription factors TFIIIB and TFIIIC and RNA polymerase III. tDNAs are
68 short, highly transcribed DNA sequences [21] that are usually nucleosome-free with
69 strongly positioned flanking nucleosomes [22-25]. The tDNAs contain internal promoter

70 elements called A and B-boxes, which aid in the binding of the transcription factor
71 TFIIIC [26, 27]. TFIIIC helps recruit TFIIIB to AT rich sequences upstream of the tDNA.
72 tDNA-bound transcription factors function via interactions with cofactors. tRNA genes
73 are sites of binding for numerous chromatin proteins including the architectural SMC
74 proteins, nuclear pore proteins, chromatin remodelers and histone modifiers. Studies
75 from several labs have shown that tDNAs are enriched in cohesin (Smc1/Smc3) [28],
76 and condensin (Smc2/Smc4) complexes [29, 30], as well as the SMC loading proteins
77 (Scc2/Scc4) [31, 32] and some chromatin remodelers including RSC [22, 29, 33-35].

78 While individual tRNA genes turn over rapidly as a result of mutational inactivation
79 and gene loss [36-38], a subset of tDNA are syntenic with respect to neighboring
80 sequences [39, 40] and data suggest that these conserved tDNAs possess
81 chromosome position-specific functions in gene regulation (reviewed in [41, 42]). There
82 are several position-specific effects mediated by tDNAs. First, tDNAs have been shown
83 to function as heterochromatin barrier insulators, which stop the spread of
84 heterochromatic domains into adjacent non-silenced domains [35, 39, 43, 44]. Second,
85 tDNAs block communication between enhancers and promoters when located between
86 these elements in yeast, *Drosophila*, mouse and human cells by acting as enhancer
87 blockers [39, 45-50]. Third, the presence of a tDNA in close proximity to a RNA pol II
88 transcribed gene promoter antagonizes transcription from the pol II transcribed gene in
89 a phenomenon referred to as tRNA gene mediated silencing (tgm silencing) [30, 51,
90 52].

91 In many organisms, tDNAs have also been shown to cluster at sites in the nucleus
92 [39, 42, 53-55]. In *S. cerevisiae*, DNA FISH studies have shown that some tDNAs

93 cluster together adjacent to centromeres [52, 54] while proximity ligation analysis
94 suggest that tDNAs cluster at the outer periphery of the nucleolus as well as near the
95 centromeres [10] though more recent HiC studies seem unable to detect these long-
96 range associations [56]. Based on these results it has been proposed that TFIIIC
97 binding to discrete sites along the chromosome plays an important role in chromosome
98 folding and organization in the yeast nucleus [54, 57, 58].

99 To better analyze the role of tDNAs in chromatin looping and organization we
100 generated a “tDNA-less” chromosome through the systematic deletion of all the tDNAs
101 on chromosome III in *S. cerevisiae*. We characterized chromatin packaging,
102 chromosome folding and nuclear dynamics of this chromosome. We show that tDNA
103 loss affects nucleosome positioning and loading of SMC proteins in the vicinity of tDNAs
104 but this has no effect on chromatin looping. While loss of the tDNAs does not affect
105 chromatin looping, it does affect centromere clustering and the long-range interactions
106 of the silenced *HML* and *HMR* loci with concomitant effects on gene silencing.

107

108 **Results**

109 The ~275 tDNAs in the budding yeast genome are dispersed across all 16
110 chromosomes. Here, we focus on chromosome III, which is 316 kb long and has two
111 tDNAs on the left arm and eight tDNAs on the right arm. In order to investigate the role
112 of tDNAs in chromatin looping, nuclear organization and function, we created a strain in
113 which chromosome III is devoid of any functional tDNAs by deleting an internal fragment
114 of each tDNA. The deletions eliminate the internal promoter elements (both BoxA and
115 BoxB) and thus eliminate the binding of the transcription factors TFIIIC and TFIIIB. For
116 simplicity, we have labeled the tDNA adjacent to the *HMR* locus as t0 and have labeled
117 the remaining nine tDNAs going from right to left as t1, t2, t3 etc. To delete the tDNAs
118 we first replaced an internal segment of the gene with a *URA3* gene and then
119 subsequently replaced *URA3* with a DNA fragment containing a unique DNA barcode.
120 This involved multiple sequential transformations. Each deletion was monitored by PCR
121 analysis, and intermediate strains were backcrossed to wild type W-303 prior to
122 additional rounds of transformations. All of the experiments described were performed
123 in this strain background to avoid strain specific effects.

124 Most tRNA isoacceptor families have multiple copies, scattered throughout the
125 genome, though single gene copies code for six isoacceptor families. On chromosome
126 III eight of the ten tDNAs that were deleted are members of multi-copy gene families
127 (with 10-16 copies in the genome) and are not essential. However, tDNA t1 (*tS(CGA)c*)
128 is a single copy gene and is essential in *S. cerevisiae* [59] and there are only two copies
129 of tDNA t7 (*tP(AGG)c*) in the genome. Loss of t7 from chromosome III caused cells to
130 grow more slowly. In order to remove these two genes from chromosome III and

131 simultaneously maintain the health of the yeast, we integrated single copies of these
132 two genes on chromosome XV at the *HIS3* locus. Once the full tDNA deletion
133 chromosome III had been constructed, the strain harboring this chromosome was
134 backcrossed with wild-type W-303, and segregation of the deleted tDNAs was
135 monitored by PCR using primers specific to the unique barcodes. The sequence of this
136 modified chromosome is available.

137 The strain where chromosome III lacked any tDNAs (tDNA delete) was grown in
138 rich media at 30C and did not show any obvious growth defect, forming homogeneous
139 and healthy, smooth edged colonies. Strains bearing this tDNA-less chromosome had a
140 doubling time of ~90 minutes in liquid YPD media, which was indistinguishable from a
141 wild type strain. This is consistent with data showing that loss of one copy of multi-copy
142 tDNAs in yeast cells do not lead to growth defects in rich media [60].

143 We analyzed the wild type and tDNA mutant strain for sensitivity to various stresses.
144 We grew haploid cells on plates containing increasing concentrations of hydroxyurea,
145 benomyl and caffeine. This analysis showed that the tDNA delete strain was as
146 resistant to these drugs as the wild type cells (Figure 1).

147 **Changes to the local nucleosome landscape surrounding the tDNAs**

148 The stable binding of TFIIC and TFIIB as well as their interactions with chromatin
149 remodelers result in nucleosome eviction at the tDNA and positioning of nucleosomes
150 adjacent to the gene [22, 61]. At some tRNA genes a single nucleosome appears to be
151 disrupted while at other tDNAs multiple nucleosomes are disrupted. Since tDNAs are
152 dispersed across the chromosome and are highly transcribed, we first asked if loss of all
153 ten tDNAs from the chromosome altered the nucleosome and transcription landscape of

154 the chromosome. In order to determine if tDNAs affect nucleosome positions across
155 chromosome III, we mapped nucleosomes in our tDNA delete strain as well as in the
156 wild type strain.

157 Haploid yeast cells were grown to log phase, harvested and nuclei were digested
158 with varying concentrations of micrococcal nuclease to generate mono-nucleosome
159 protected DNAs, which were subjected to paired-end MNase-seq. Overall, the
160 nucleosome landscape across all chromosomes except chromosome III was unaffected
161 by the presence or absence of the chromosome III tDNAs. More focused analysis
162 showed no change in nucleosome positioning in the proximity of the 265 tDNAs
163 scattered on the 15 chromosomes that were not manipulated in this study (Figure 2A).

164 In contrast, changes in nucleosome occupancy were observed at or immediately
165 adjacent to the deleted tDNAs on chromosome III. Figure 2B shows the average
166 nucleosome occupancy across 2kb segments centered on the chromosome III tDNAs
167 with each tDNA in WT cells aligned at its 5' end while in the tDNA delete strain, the 5'
168 ends of the deletion points were aligned. In the wild type strain there is a clear
169 nucleosome free region centered on the tDNA flanked by positioned nucleosomes
170 reflecting differential digestion of the TFIIB-TFIIC complex relative to nucleosomes [35,
171 62]. In the tDNA delete strain this pattern is altered and a nucleosome is usually formed
172 over the deletion junction (see Figure2D). We were unable to determine the change in
173 the chromatin landscape around t1 and t7 tDNAs since these two genes with 100 bp of
174 flanking sequences were transposed to the *HIS3* locus. Nucleosome positions
175 elsewhere on chromosome III that are distant from the tDNAs are not altered on the
176 tDNA-less chromosome (Figure 2C). These results demonstrate that tDNAs create

177 nucleosome free regions at the tRNA gene with positioned nucleosomes flanking the
178 gene. The data also show that their chromatin organizing effects are locally confined
179 and do not extend beyond their immediate vicinity.

180 **tDNA loss affects expression of few RNA pol II transcribed genes**

181 The presence of a tDNA in close proximity to a RNA pol II transcribed gene promoter
182 antagonizes transcription from the pol II transcribed gene called tRNA gene mediated
183 silencing (tgm silencing) [30, 51, 52]. In addition, tDNAs have also been shown to
184 function as enhancer blockers when located between an UAS enhancer and a promoter
185 [47]. Since the loss of the tDNAs altered nucleosomes in their vicinity we wondered if
186 these alterations affected the transcription landscape of genes on chromosome III.
187 Rather than restrict the analysis to pol II transcribed genes adjacent to the tDNAs on
188 chromosome III, we investigated the effects of tDNA loss on all pol II transcribed genes
189 in the genome and analyzed the changes in RNA levels in the wild type and tDNA
190 delete strain by RNA-seq. Total RNA was extracted from exponentially growing yeast
191 cultures and RNA-seq libraries were prepared, sequenced and analyzed as described in
192 the materials and methods section. The RNA levels of a very small number of genes
193 were affected upon deletion of the tDNAs. Table1 lists the genes that were either up
194 regulated or down regulated in the strain lacking tDNAs on chromosome III. Of the ten
195 tDNAs present on chromosome III, tDNA t0, t8 and t9 are flanked by retrotransposon
196 elements and since these are repetitive elements, the tDNA-mediated transcription
197 effects could not be investigated for these loci. Furthermore, tDNAs t3 and t4 are
198 missing in W-303. The expression of only two genes on chromosome III was affected
199 and in both instances, a tDNA (t1 and t6) was located adjacent to the gene. In one

200 instance the gene was up regulated upon tDNA loss while in the second instance the
201 gene was down regulated. Furthermore, we observed the up regulation of the *MRM1*
202 gene. This gene resides immediately adjacent to *HIS3*. The tDNAs for t1 and t7 were
203 ectopically inserted at the *HIS3* locus in the tDNA delete strain demonstrating that the
204 ectopic insertion of the tDNAs is the cause of the change in expression of *MRM1*. These
205 data suggest that tDNA mediated position effects are highly context dependent and only
206 affect some pol II transcribed genes and not others.

207 Of the genes that were down regulated in the tDNA delete strain, several are
208 involved in amino acid biosynthesis though these genes are scattered throughout the
209 genome and do not localize near tDNAs. The reason why expression of these genes
210 was reduced is unclear given that the two yeast strains used are isogenic with respect
211 to nutritional markers, and there are between 10 and 16 copies of each of the six
212 deleted tDNAs in the genome (t0=11 copies, t2=10 copies, t5=16 copies, t6=11 copies,
213 t8=10 copies and t9=15 copies). It is possible that there is a reduction in transcript
214 levels of these genes due to the small reduction in tDNA copy number without any other
215 cell phenotype. This is consistent with a recent study where single tDNAs in yeast were
216 deleted and these single deletions in multi-copy tDNA families also led to changes in the
217 expression of a small set of genes involved in translation [60].

218 **Scs2 binding at tDNAs is dependent upon a functional tDNA but other binding**
219 **sites are tDNA independent**

220 The SMC proteins play an important role in nuclear organization [63] and tDNAs are
221 major binding sites for SMC proteins and the SMC loaders Scs2/Scs4 and Rsc. Our
222 nucleosome mapping data indicated that loss of the tDNAs altered nucleosome

223 positions at tDNAs. Since nucleosome free tDNAs are sites for the recruitment of RSC
224 and Scc2/Scc4 proteins [31, 34, 64, 65], we asked if loss of all the tDNAs on
225 chromosome III reduced recruitment of Scc2 proteins at these loci and whether it also
226 affected loading of Scc2 at other sites along the chromosome.

227 We performed a ChIP-seq of Myc-tagged Scc2 to compare the distribution of this
228 protein genome wide in the WT and tDNA delete strain (Figure 3). This analysis showed
229 Scc2 binding at multiple sites along the chromosome including tDNAs. At some tDNAs
230 the Scc2 binding is focused forming a sharp peak while at other tDNAs the binding is
231 spread over a greater region. Comparison between the wild type and tDNA delete strain
232 showed that Scc2 levels did not decrease at any of the sites on the 15 chromosomes.
233 Upon tDNA loss Scc2 binding decreased at the tDNA loci on chromosome III or at sites
234 in the immediate vicinity of tDNAs such as *LEU2* (adjacent to tDNA t8) (Figure 3) and
235 *HMR* (adjacent to t0). On chromosome III the analysis also showed that there was no
236 significant change in Scc2 binding at other non-tDNA sites on chromosome III. For
237 example we saw a large peak of Scc2 binding at Tel3L. This peak at Tel3L was
238 unchanged upon tDNA deletion and similarly we did not record any change in Scc2
239 levels at *CEN3* confirming that tDNAs are not the sole determinants for the recruitment
240 of Scc2 to chromosomes.

241 We confirmed this result by ChIP-qPCR against Scc2. A site at the *OCA4* gene was
242 used as an internal control since this site does not bind Scc2 in wild type cells. We were
243 unable to design unique primers at t6 due to the presence of repetitive sequences in the
244 immediate vicinity of this gene and therefore could not map the localization of these
245 proteins at this tDNA. Some primer pairs flank the tDNAs while others are adjacent to

246 the tDNAs. Consistent with the ChIP-Seq data, in wild type cells, Scc2 is enriched at
247 several of the tDNAs present on chromosome III (Figure 4A). We observed ~3.5 fold
248 enrichment at t8 and ~2.5 enrichment at t0, t2 and t5. When the same protein was
249 mapped in the tDNA delete strain we observed a significant reduction in Scc2 binding at
250 these tDNAs. The levels dropped to those observed for the negative control *OCA4*
251 except for the t8 tDNA, where the level dropped two fold but there was some residual
252 Scc2 still present (Figure 4A). The amount of Scc2 did not change at *CEN3* when the
253 tDNAs were absent from the chromosome, indicating that the binding of Scc2 to the
254 centromere was independent of the tDNAs.

255 Scc2, in association with Scc4 helps recruit the SMC proteins to chromatin [29, 32].
256 Condensins localize to tDNAs and are necessary for the clustering of tDNAs in the
257 nucleus [29, 30]. We therefore mapped the binding of condensins at tDNAs on
258 chromosome III using the HA-tagged Brn1 subunit. In wild type cells, the Brn1 profile
259 was very similar to that previously observed for Scc2 with significant binding of Brn1 at
260 specific tDNAs. Correspondingly, the binding of the condensins was significantly
261 reduced at these sites upon deletion of the tDNA promoters (Figure 4B).

262 **Chromosome mobility on the tDNA-less chromosome**

263 TFIIC binding sites and tDNAs are described as chromosome organizing clamps
264 because of their consistent association with specific landmarks within the nucleus [54].
265 The localization of tDNAs with the kinetochore is dependent upon condensins while the
266 interactions of tDNAs with nuclear pores in the G2 phase of the cell cycle are dependent
267 upon cohesins. These associations likely help tether the chromosome. Since loss of
268 tDNAs from chromosome III led to a decrease in SMC proteins from these sites we

269 wondered if this loss would affect chromosome tethering and mobility of the
270 chromosome. To assess mobility we fluorescently-labeled specific sites on chromosome
271 III, and used these to monitor chromosome mobility in the wild type and the tDNA
272 deletion chromosomes. The location of a point on the chromosome was mapped in
273 three-dimensional space over a defined period of time in relation to another point within
274 the nucleus- the spindle pole body (marked with the Spc29-RFP fusion protein)- and
275 mobility was characterized by mean square distance analysis (MSD) as described
276 previously [66-68]. Six chromosomal loci across chromosome III were assayed (Figure
277 5). These loci were tagged by inserting LacO arrays at these sites and monitored using
278 a LacI-GFP fusion protein mediated fluorescence. Time-lapse movies of >35 individual
279 unbudded cells (in the G1 phase of the cell cycle) were imaged over the course of 10
280 minutes. Z-stack images of the cells were taken every 30 seconds during the time-
281 lapse, and MSD was calculated at each time-point using the following equation: $\langle (X_t - X_{t+\Delta t})^2 \rangle$.
282 Using this information, MSD curves were generated for each locus in both the
283 WT and tDNA delete strain (data not shown). For the wild type chromosome III, *CEN3*
284 was the most constrained locus ($R_c=415$ nm), with loci located further from the
285 centromere exhibiting greater mobility. For example, *LEU2*, which is approximately 30kb
286 from the centromere, had an R_c of 522nm while *HMR*, which is approximately 180kb
287 from the centromere, had an R_c value of 688nm. This is consistent with previous data
288 showing that the location of a locus in relation to the centromere is critical in determining
289 its mobility, with loci closer to the centromere displaying decreased mobility compared
290 to loci farther from the centromere [9, 68, 69]. Comparison of mobility of segments in the
291 wild type and tDNA delete strains, showed a small decrease in mobility in the tDNA

292 delete strain at a couple of sites (*SRO9* and *CEN3*). However these differences were
293 not statistically significant (p values= 0.15 and 0.19). The data indicate that tDNAs are
294 not major determinants in constraining chromosome arm motion or that they are a
295 subset of factors involved and the redundancy precludes observation of their
296 contribution.

297 **tDNAs are not required for proper chromatin folding**

298 Transfer RNA genes have been proposed to affect chromatin fiber folding via the
299 clustering of dispersed tRNA genes. The promoters in tDNAs are the binding site for the
300 transcription factor TFIIIC and foci comprised of multiple TFIIIC-bound sites have been
301 proposed to function in chromatin looping and folding [10, 39, 52-54, 57, 58, 70]. If
302 tDNAs are major drivers of chromatin folding and looping, then elimination of these loci
303 from an entire chromosome should lead to changes in the folding of the chromatin fiber
304 or result in changes in chromosome packaging in the nucleus. We set out to determine
305 the detailed three-dimensional organization of chromosome III lacking functional tDNAs.
306 We used a modified chromosome conformation capture technique called Micro-C XL
307 [71, 72]. We chose Micro-C XL over HiC because it can capture both short length 3D
308 interactions as well as some long-length interactions and the method is not dependent
309 upon the distribution of restriction sites along the DNA. In brief, yeast cells were first
310 cross-linked with formaldehyde and DSG, and chromatin was then fragmented into
311 mono-nucleosomes via micrococcal nuclease digestion. Cross-linked, digested
312 chromatin was ligated to capture chromosomal interactions. Size-selected ligation
313 products were then purified and subjected to paired-end high-throughput sequencing.
314 Sequencing reads were mapped back to the reference genome to determine the

315 interacting regions of the chromosome, as previously described. For each strain two
316 independent cross-linking and ligations were performed and QuASAR (Quality
317 Assessment of Spatial Arrangement Reproducibility) and Genome DISCO (Differences
318 between smoothed contact maps) were used to assess the reproducibility of the data.
319 The two independent measurements both gave a score >95% confirming the
320 reproducibility between the two biological replicates for the wild type and tDNA delete
321 strain. Reproducibility of the data was also analyzed by measuring contact probability
322 over genomic distance and the decay curves between replicates overlapped almost
323 completely which is consistent with our reproducibility measurements.

324 Overall, Micro-C maps for wild type and tDNA mutant strains both exhibited
325 previously described features of yeast chromosome folding, with no difference in
326 chromatin folding between the tDNA delete and wild type strains. The chromatin
327 interaction maps of chromosome IX show that most Micro-C interactions occurred close
328 to the diagonal in both strains though there was significant variation in the density along
329 the diagonal. The data clearly show ~2-10kb contact domains (CIDs/TADs)
330 encompassing ~1-5 genes in both strains (Figure 6A). We calculated the insulation
331 score across bins and a scatter plot of the insulation scores for wild type and mutant
332 strains is consistent with the conclusions that the overall architecture of chromosomes
333 in these two strains was not altered (Figure 6B).

334 Inspection of the chromosome III in the wild type and tDNA delete cells showed that
335 these interaction domains persisted on this chromosome even upon loss of the tDNAs
336 from chromosome III. The interaction decay curve for chromosome III is very similar in
337 the wild type and tDNA delete strain indicating that the overall folding of the

338 chromosome has not altered (Figure 6C). There was no significant change in the
339 contact frequency versus genomic distance in the two strains, indicating no local
340 chromatin decondensation or change in chromatin looping interactions.

341 We analyzed the contact frequency of sites immediately adjacent to the 8 tDNAs on
342 chromosome III in the wild type and tDNA delete strains. At some sites, the loss of the
343 adjacent tDNA did not alter long-range interactions at all while at other sites there was
344 small changes though the significance of these remains to be elucidated (Figure 6D).

345 Thus, tDNAs do not appear to be responsible for the general folding of the chromatin
346 fiber and the CID/TAD architecture.

347 **tDNAs affect CEN-CEN interaction frequency**

348 While the overall folding of the chromatin fiber of chromosome III was not altered
349 micro-C analysis identified changes in contact frequency at specific sites along
350 chromosome III. In order to identify sites where contact frequency had changed the
351 contact maps were normalized by distance for the wild type and tDNA delete strains
352 (Figure 7A). These matrixes were used to identify differential contact sites (generated
353 by dividing the tDNA delete matrix by the wild type matrix). This analysis identified
354 increased sites of contacts in the tDNA delete strain (shown in red) around the
355 centromere and near the telomeres of chromosome III (Figure 7B).

356 The 16 centromeres in yeast are in close physical proximity to one another and
357 cluster adjacent to the spindle pole body [7, 73, 74]. These CEN-CEN interactions are
358 readily captured by 3C methods including HiC [10, 71, 75], and are recapitulated in this
359 study in the W-303 strain background. Interestingly compared to the wild type strain, the
360 centromere of chromosome III in the tDNA delete strain showed an increased frequency

361 of interactions with the other centromeres. Focusing on the 50kb pericentric region of
362 each chromosome, we found that most CEN-CEN interactions were minimally affected
363 by the loss of chromosome III tDNAs. For instance, interactions between the
364 chromosome XVI centromere and the remaining centromeres showed that interactions
365 between *CEN16* with the majority of centromeres remained unchanged, but that there
366 was a ~20% increase in interaction strength between *CEN16* and *CEN3* when
367 chromosome III lacked tDNAs (Figure 7C).

368 This increase in *CEN3* interaction was not confined to *CEN16*. When the same
369 analysis was performed using *CEN3* as an anchor, we observed increased frequency of
370 interactions between *CEN3* and all of the other chromosomal centromeres in the tDNA
371 delete strain (Figure 7D). Most of the interaction counts increased approximately 20%
372 compared to WT, with the highest increase seen at *CEN3-CEN9*. The increase in the
373 *CEN3-CEN* interactions in the tDNA deletion strain was significantly higher ($p=1.22 \times 10^{-14}$)
374 compared to values of all *CEN16-CEN* interactions (excluding *CEN16-CEN3*). These
375 results show that upon deletion of all tDNAs across chromosome III, inter-chromosomal
376 interactions increase between *CEN3* and the other centromeres, suggesting that
377 functional tDNAs likely antagonize CEN-CEN associations during interphase.

378 We next measured chromosome loss rates of wild type and tDNA delete diploid
379 cells. We first constructed homozygous diploid cells containing *URA3*, *TRP1* and the
380 *MAT* locus located on chromosome III (in both the wild type and tDNA delete strain).
381 Single diploid colonies were grown for 20 doublings in YPD and approximately 10^7 cells
382 were plated onto 5-FOA plates to measure the number of cells that had become *URA3*
383 negative. Cells could have become uracil auxotrophs by gene mutations or via loss of

384 the chromosome. These two types of mutants could be distinguished by replica plating
385 the 5-FOA resistant colonies onto plates lacking tryptophan or by checking for the
386 appearance of MAT α pseudo haploid cells. The number of cells unable to grow on
387 media lacking tryptophan and also being able to mate were counted and chromosome
388 loss rates were calculated by dividing the number of these colonies by the total number
389 of cells plated. In wild type cells the loss rate for chromosome III was 4.08×10^{-5} and is in
390 agreement with previous reports [76]. The loss rates for the tDNA delete chromosome
391 decreased slightly to 3.26×10^{-5} suggesting that loss of the tDNA slightly helped stabilize
392 the chromosome ($p=0.02$).

393 **tDNAs play a role in *HML-HMR* long-range association**

394 The silent loci *HML* and *HMR* reside on chromosome III separated by approximately
395 300kb along the linear chromosome. However, the *HML* locus, located 11kb from
396 *TEL3L*, is in close three-dimensional proximity to the *HMR* locus, located 23kb from
397 *TEL3R*. This long-range interaction has previously been detected using both live-cell
398 microscopy and HiC analysis [20, 75, 77] and we recapitulate this finding in the Micro-C
399 experiment with the wild type strain (Figure 8A). Comparing wild type cells to the tDNA
400 delete strain, we noticed that the interaction of *HML* with *HMR* was slightly altered in the
401 tDNA delete strain. In wild type cells, there was an interaction between *HML* and *HMR*
402 and this interaction zone became less defined and more diffuse upon deletion of the
403 tDNAs and a slightly increased interaction frequency was observed across a broader
404 region of the end of chromosome III. While *HMR* still interacted with *HML* in the deletion
405 strain, it appeared to also display interactions with other loci (including *TEL3L*).
406 Similarly, the segment containing *HML/TEL3L* showed increased interactions with

407 *TEL3R* rather than being restricted to interacting with sequences at *HMR*. These results
408 suggest that deletion of chromosome III tDNAs subtly perturbed *HML-HMR* long-range
409 interactions.

410 Given that Micro-C measures population averages of stable long-range interactions
411 we decided to measure *HML-HMR* interactions in live cells using fluorescence
412 microscopy. We wished to determine if the tDNAs influenced *HML-HMR* interactions.
413 We generated a strain with multiple Lac operator sequences inserted adjacent to *HMR*
414 (at the *GIT1* gene) and multiple copies of the Tet operator sequences inserted adjacent
415 to *HML*. Expression of the fusion proteins CFP-LacI and YFP-TetR in this strain enabled
416 us to visualize these loci in living yeast by fluorescence imaging. The distance between
417 *HML* and *HMR* was then measured in wild type and a strain lacking the t0 tDNA (Figure
418 8B). We found that in wild type cells, *HML* was in close proximity to *HMR*. Consistent
419 with our expectations, deletion of Sir proteins resulted in separation of these loci
420 validating this assay. Importantly, when we eliminated the t0 tDNA, this led to a change
421 in the distance between *HML* and *HMR* compared to wild type cells, with the median
422 distance between *HML* and *HMR* increasing upon deletion of the tDNA. Given the
423 presence of outliers in the data we used a Mann-Whitney U-Test to determine statistical
424 significance between wild type and the mutant. With an n of approximately 300 cells for
425 the wild type and tDNA delete strain we observed a p value of 3.1×10^{-14} showing that the
426 differences observed between the two strains were significant. Closer analysis of the
427 plot indicates that upon deletion of the tDNA there is heterogeneity in the distances
428 between the two loci and a continuum of values. Thus there are cells where the two loci
429 are in very close proximity as well as cells where the two loci are further apart. It should

430 be noted that the HiC approach and the microscopic method to measure proximity are
431 inherently different and distinct and each method provides different types of information
432 and each approach has specific limitations. Use of long arrays bound tightly by
433 repressor proteins that dimerize may influence chromatin architecture and fluorescence
434 measurements [78]. Similarly the HiC based methods are influenced by indirect
435 crosslinking especially in regions of condensed heterochromatin and nuclear
436 substructures like sites near centromeres and the nuclear envelope [79-81].

437 The tDNA t0 is necessary for the recruitment of cohesins to the silenced loci and the
438 SMC proteins are necessary for long-range *HML-HMR* interactions [20]. However not all
439 tDNAs are equivalent in their ability to recruit cohesins to the silenced loci [43, 82, 83].
440 We therefore inquired if tDNAs that are unable to recruit cohesins are able to restore
441 long-range association between *HML* and *HMR*. We replaced the *HMR* tDNA^{THR} (t0)
442 with tDNA^{THR} (NL1) from chromosome XIV. This tDNA has identical sequence to the t0
443 tDNA in the body of the gene and therefore has the identical BoxA and BoxB promoter
444 sequence and spacing as tDNA t0. However sequences flanking this tDNA are distinct
445 and the NL1 tDNA is unable to recruit/bind cohesins [82, 83]. The NL1 tDNA has
446 reduced binding of TFIIC and a narrower nucleosome free region as well [62, 84]. This
447 tDNA also has reduced nucleoporin binding and reduced histone turnover frequency
448 [61, 85]. When we replaced a 300bp t0 tDNA-containing fragment with a 300 bp NL1
449 tDNA-containing fragment we found that the NL1 tDNA was not able to robustly restore
450 long-range *HML-HMR* interactions, suggesting that tDNA mediated local chromatin
451 organization might be necessary for these long-range interactions.

452 **Replication fork pausing at tDNA mediates long-range chromosomal**

453 **interactions**

454 We had previously shown that DNA double strand repair proteins help deposit
455 cohesins to the silenced loci, which then lead to homology dependent long-range
456 interactions between *HML* and *HMR* [19, 20]. Since we had discovered that a specific
457 tDNA helped in the clustering of *HML* and *HMR*, we wished to know the mechanism by
458 which this phenomenon occurred. Replication fork pausing/stalling is observed at many
459 tDNAs. This results in the deposition of γ -H2A at the tDNA and this is necessary for fork
460 recovery from the pause/stall [20, 29, 86-90]. Rrm3 and topoisomerases play a role in
461 the recovery of stalled replication forks at protein bound sites in the genome such as
462 tDNAs [88, 91, 92]. Therefore we analyzed the effect of these mutants on *HML-HMR*
463 long-range association. The data show that deletion of Rrm3 as well as mutants in the
464 DNA polymerase- ϵ subunit Dpb3 and the topoisomerase Top1 lead to a statistically
465 significant decrease in *HML-HMR* long-range association (Figure 5B and figure legend).
466 Thus the presence of a tDNA as well as normal Rrm3, Top1 and Dpb3 function are
467 necessary for the establishment or maintenance of the long-range association between
468 *HML* and *HMR*.

469 **tDNA enhances epigenetic gene silencing at clustered *HML-HMR***

470 Since the tDNA is necessary for the long-range clustering of the silenced domain,
471 we wondered if reduction in clustering had any effect on gene silencing. We asked
472 whether tDNA mediated loss of *HML-HMR* interactions affected gene silencing at *HML*
473 and *HMR*. Silencing can be assayed by insertion of reporter genes within or
474 immediately adjacent to the silenced domains. In wild type yeast when a reporter gene

475 is inserted immediately adjacent to these loci, the gene is metastably silenced. A
476 cassette containing an H2B (*HTB1*) promoter driving *HTB1-EYFP* was integrated to the
477 right of *HML* while a cassette containing the *HTB1* promoter driving *HTB1-ECFP* was
478 integrated to the left of *HMR*. In addition, on chromosome XV, a cassette containing an
479 *HTB1* promoter driving *HTB1-mCherry* was integrated as a control euchromatic marker
480 [93]. The *HTB1-mCherry* gene is active in all cells in the population. The *HML::YFP* and
481 the *HMR::CFP* reporter genes are present immediately outside of *HML* and *HMR* but
482 reside in a region bound by Sir proteins [4, 22]. These genes adopt one of two
483 expression states, either active or silent. For visualization, single cells were placed on
484 microfluidic plates and monitored continuously by fluorescence microscopy. Fluorescent
485 signal from each individual cell was recorded every 40 minutes over a period of ~24
486 hours. This allowed us to trace the lineage of each daughter from the founder cell and
487 score the cells according to the expression of the reporter genes at *HML* and *HMR*. Cell
488 lineage trees were traced and each cell in the lineage was assigned a positive or
489 negative value for expressing each reporter as it underwent cell division (Figure 9A).

490 We initially analyzed the silencing of the reporter genes in the wild type strain.
491 Consistent with previous data [93], reporters at *HML* and *HMR* were regulated such that
492 the reporters maintained their activity state over many generations and occasionally
493 switched to the opposite expression state. Once they switched they maintained the new
494 state for several generations. Furthermore, when one reporter was active the other was
495 also more likely to be active suggesting long-range coordination between *HML* and
496 *HMR* though this coordination is not absolute.

497 We next investigated silencing of the reporters in a strain where chromosome III
498 lacked all the tDNAs. In this strain, the reporter at *HMR* was active more often
499 compared to the wild type strain. While the effect was not as pronounced, the same
500 effect was also observed at *HML* (Figure 9A tDNA delete panel). Furthermore, the
501 silenced state was less stable, and switched to the active state more often. This
502 suggests that silencing at these loci is influenced by the tDNAs.

503 While expression states at both *HML* and *HMR* were stably inherited, the
504 transcriptional state did flip in daughter cells (Figure 9B). An expressed to repressed
505 transition was a less frequent event compared to the repressed to expressed transitions
506 regardless of genotype. This is not entirely surprising since the reporter genes were
507 inserted immediately outside of the two silencers in a zone where the silent state is
508 metastable [94, 95]. However, when analyzing the repressed to expressed transitions,
509 we saw a discernible difference in the frequency of the expression of the reporter genes
510 at *HMR*. The full tDNA delete strain showed an increased frequency of cells undergoing
511 the transitions at *HMR* compared to wild type cells and the inverse was seen for the
512 expressed to repressed transition (Table 4).

513 Given that the transcription states of the reporters were affected at both *HML* and
514 *HMR* in a strain containing full tDNA deletions on chromosome III even though only
515 *HMR* has a tDNA adjacent to it, we decided to focus on the tDNA (t0) that resides
516 immediately adjacent to *HMR* and functions as an insulator at *HMR*. Importantly, t0 lies
517 to the right of *HMR* while the reporter gene lies to the left of *HMR*, so any effect of t0 on
518 the transcriptional state of the reporter is not due to the barrier function of this tDNA.

519 To test whether *t0* is necessary for regulating silencing states at *HML* and *HMR* we
520 built a strain where only *t0* was deleted on chromosome III (*t0*⁻). The lineage tree
521 showed that this strain behaved similarly to the strain lacking all tDNAs such that both
522 reporters were active most of the time and rarely switched to the repressed state. Like
523 the full tDNA delete, the *t0*⁻ strain showed an increased frequency of cells undergoing
524 the transitions at both *HML* and *HMR* when compared to the wild type strain where a
525 reporter gene that was not expressed in one generation was more likely to be
526 expressed in the next generation.

527 Alternatively, to determine if the *t0* tDNA was sufficient for mediating silencing
528 effects at *HML* and *HMR*, we constructed a strain lacking 9 of the 10 tDNAs on
529 chromosome III and where *t0* is the only tDNA still present at its normal location
530 adjacent to *HMR* (*t0*⁺). Again, we monitored expression of the reporters at *HML* and
531 *HMR* in this background. The lineage tree showed that this strain behaved similarly to
532 the wild type strain such that both reporters were silent more often than the full tDNA
533 delete and *t0*⁻ strains and inherited the silent state with greater fidelity.

534 Taken together, the data suggest that deletion of tDNAs on chromosome III had an
535 effect on the ability of *HMR* to interact with *HML* and diminution of this clustering led to
536 an alteration in the stability of the silenced state at these loci.

537

538

539

540

541 **Discussion**

542 tDNAs are middle repetitive DNA sequences scattered across all 16 chromosomes
543 and their primary function is the synthesis of tRNAs. In this manuscript, we show that
544 tDNAs affect local chromatin structure, which then impinges on chromosome
545 architecture. tDNAs 1) affect chromatin structure by maintaining local nucleosome free
546 regions along the fiber and precisely positioned nucleosomes immediately outside of the
547 tDNAs, 2) recruit cohesins and condensins 3) affect nuclear architecture by influencing
548 centromere clustering and 4) alter heterochromatin clustering leading to changes in the
549 fidelity of inheritance of gene silencing.

550 The binding of specific proteins such as CTCF to a site on the DNA can affect
551 nucleosome positions over long distances [96]. Nucleosome depletion at the gene and
552 positioned nucleosomes flanking the gene is a hallmark of tDNAs [22, 24, 25, 35, 61,
553 97-100]. Our data show that loss of the tDNA promoters' only affect nucleosome
554 positions in the immediate vicinity of the tDNA. The nucleosome positioning effects
555 mediated by the tDNA bound transcription factors TFIIIC and TFIIIB are not transmitted
556 over long distances.

557 **tDNAs, SMC proteins and chromatin folding**

558 The SMC proteins are involved in higher order chromosome organization in all
559 eukaryotes and have been extensively mapped. tDNAs are binding sites for all three
560 classes of SMC proteins (cohesin, condensin and repairsin), the SMC protein loaders
561 Scc2 and Scc4 and the meiotic Rec8 SMC protein [28, 29, 32, 101-105]. Given these
562 intimate connections between tDNAs and the SMC proteins our data indicate that loss
563 of the tDNA promoters does lead to loss of SMC proteins from tDNAs but this effect is

564 tDNA specific since we do not see a loss of SMC proteins from centromeres or Scc2
565 from other sites in the genome. Surprisingly the loss of Scc2 and Brn1 from tDNAs does
566 not affect chromatin folding. While clustering of tDNAs in the nucleus (as measured by
567 fluorescence microscopy) is dependent upon the SMC proteins [54, 70] the precise
568 contribution of tDNAs in this process remained unclear. Our Micro-C analysis suggests
569 that tDNAs play a minor role in chromatin folding and tethering to nuclear substructures
570 since we observed only subtle changes in contact frequency across the chromosome
571 and small effects on chromosome loss rates. It is likely that tDNA independent SMC
572 protein binding sites masks the tDNA-mediated effects. SMC proteins bind only half of
573 the tDNAs in the nucleus and only a third of the SMC protein binding sites localize at or
574 near tDNAs [29]. The lack of phenotype would also be consistent with previous data that
575 showed that a reduction in the levels of the SMC proteins does not affect the properties
576 of the chromosome arm [106]. Recently a synthetic yeast chromosome III was
577 generated and characterized [107, 108]. The synthetic chromosome lacks repetitive
578 sequences such as TY elements, LTRs and tRNA genes. The 3D structure of this
579 chromosome was determined using HiC and the data show that there were no major
580 differences between this chromosome and the wild type chromosome except for a
581 shortening of the length. While this chromosome lacks multiple elements the three-
582 dimensional folding data are consistent with our conclusions from the Micro-C analysis
583 of the same chromosome lacking only tDNAs.

584 While it is possible that redundancy of structural elements masks tDNA-mediated
585 effects on chromatin folding it is also possible that chromatin folding is driven by
586 underlying DNA sequence mediated nucleosome organization and not tDNA mediated

587 long-range interactions. The yeast chromosomes have isochores with G-C rich, gene
588 rich R-band segments alternating with AT-rich G-band segments [109, 110], which
589 exhibit different functional properties and chromosome conformation [111, 112].
590 Chromosome III has a G-C segment from 20 to 100 kb on the left arm followed by an A-
591 T rich central segment from 100 to 200kb on the right arm and then a second G-C rich
592 segment from 200 to 290kb on the same arm. In this scenario, the underlying A-T rich
593 DNA sequence likely plays a dominant role in the three dimensional folding of
594 chromatin. tDNAs are often syntenic along chromosomes [39, 113] and it is possible
595 that these positions have been selected for optimal gene activity rather than being
596 involved in long-range chromatin loop formation [114]. Thus while the A-T rich isochore
597 is structurally and functionally distinct [75, 115, 116] and is the region rich in tDNAs
598 (See Figure1) our results would suggest that the tDNAs do not play a significant role in
599 either tethering of this isochore or the overall folding of this segment. The tDNA
600 clustering observed by microscopy could simply be a function of conservation of tDNA
601 positions along the chromatin fiber.

602 **tDNAs and centromere clustering**

603 Chromosome tethering to nuclear substructures enables nuclear organization [1,
604 114] and centromeres and the telomeres along with their associated proteins play a key
605 role in this process [7, 9, 10, 12, 15, 16, 73, 117-120]. All sixteen centromeres cluster
606 together in a ring around the membrane-embedded spindle pole body. The centromeres
607 are tethered to the spindle pole body via direct interactions between kinetochore-
608 associated proteins and the spindle pole body associated microtubules in interphase [7,
609 73, 75, 117]. Other factors are likely to influence this phenomenon but remain unknown.

610 tDNA density is almost 2 fold higher in the pericentric region of *S. cerevisiae*
611 chromosomes including chromosome III [121]. While tDNAs have been shown to help
612 tether centromeres to the spindle axis during mitosis [121], in interphase nuclei, the loss
613 of tDNAs results in increased interactions between the clustered centromeres. The
614 physical presence of tDNAs in the pericentric region could interfere with the close
615 packaging of centromeres during interphase. This could be due to transcription-
616 mediated effects since tRNA genes are highly active. In *S. pombe*, mutations that
617 reduce tDNA transcription result in increased tDNA association with the kinetochore and
618 increased chromosome condensation during mitosis. Furthermore, tDNA association
619 with kinetochores increases when these genes became inactive [55]. Thus, tDNA
620 clustering at sites of active tRNA transcription near centromeres could hinder
621 centromere-centromere interactions during interphase while a decrease in tDNA
622 transcription during mitosis could help tether centromeres to the spindle axis during
623 mitosis [121]. This would also explain the observation that the tDNA-deleted
624 chromosome had a slightly lower chromosome loss rate.

625 An alternative though not mutually exclusive possibility is based on the observation
626 that transcriptionally active tDNAs interact with nuclear pores in the G2/M phase of the
627 cell cycle [4, 122, 123]. It is thus possible that there is a competition between pericentric
628 tDNA- nuclear pore interactions in opposition to centromere-centromere interactions. In
629 this scenario, the loss of tDNA tethering to the nuclear pore would enable the
630 centromere greater freedom of movement thus enabling closer centromere-centromere
631 interactions.

632 **tDNA effects on *HML-HMR* interactions and the inheritance of gene silencing**

633 Gene silencing is primarily a function of the Sir proteins though numerous other
634 factors influence the process [124]. Proto-silencers are sequence elements that on their
635 own are unable to silence a gene, but when located near a silencer increase the
636 efficiency of silencing [125, 126]. Our demonstration that the tDNA affects silencing of a
637 reporter adjacent to the silent *HMR* domain suggests that tDNAs function as proto-
638 silencers. Our data suggest that tDNA mediated clustering of silent loci might be
639 important in the silencing of these loci and the loss of long-range association might
640 reduce the efficient inheritance of the silent state. This is analogous to the observations
641 that gene clustering at active chromatin hubs and transcription factories increases the
642 efficiency of transcription as well as the data showing that telomere clustering increases
643 the efficiency of silencing at sub-telomeric sequences [127].

644 This unexpected observation also raises the question of how might tDNAs influence
645 long-range *HML-HMR* interactions. tDNAs, including the tDNA next to *HMR*, are sites of
646 replication slowing/pausing [86, 87, 91, 128-130]. The tDNA adjacent to *HMR* is a site
647 of replication fork pausing [89, 131]. We recently showed that long-range *HML-HMR*
648 interactions require homologous sequences to be present at these loci [19, 20] and we
649 now show that mutations in replication coupled homologous recombination repair
650 proteins including the SMC proteins, Rrm3, Top1 and Dpb3 lead to a reduction in *HML-*
651 *HMR* interactions. Based on the accumulated data we would posit that replication fork
652 slowing/pausing results in the deposition of γ H2A and SMC proteins at tDNAs followed
653 by a homology search leading to *HML-HMR* interactions. The re-formation of silenced
654 chromatin following replication precludes the eviction of γ H2A [132] thereby stabilizing
655 SMC protein binding, which then maintains the long-range *HML-HMR* association. The

656 tDNAs thus help initiate a network of interactions mediated by the SMC proteins and the
657 Sir proteins leading to *HML-HMR* association and chromosome folding. We would like
658 to posit that a series of transient interactions during replication aid in the setting up of
659 the final optimal nuclear architecture found in the interphase nucleus.

660 In conclusion, tDNAs primarily affect local chromatin structure. Each tDNA affects
661 nucleosome positions and protein binding in its immediate vicinity. These local
662 perturbations functionally and structurally interact with neighboring regulatory regions
663 resulting in tDNA mediated pleiotropic effects. In some instances tDNAs affect the
664 expression of neighboring pol II transcribed genes by the phenomenon of local tgm
665 silencing. In another context tDNA mediated replication pausing result in the
666 establishment of long-range heterochromatin interactions, which then influence the
667 inheritance of silencing states at these loci.

668 **Acknowledgements**

669 This work was supported in part by a grant from the NIH to RTK (GM078068) and (T32-
670 GM008646) to JK, OH and KW. This study was funded in part by the Intramural
671 Research Program of the National Institutes of Health (NICHD). We thank the NHLBI
672 Core Facility for paired-end sequencing of the micrococcal nuclease libraries. The
673 Functional Genomics Laboratory, UC Berkeley sequenced the ChIP-Seq libraries on an
674 Illumina HiSeq4000 at the Vincent J Coates Laboratory at UC Berkeley, supported by
675 an NIH S10 OD018174 Instrumentation Grant.

676

677 **Materials and Methods**

678 **Yeast strains and primers**

679 Table 2 and 3 list the yeast strains and the primer sequences that were used in this
680 study.

681 **MNase-Seq**

682 MNase-Seq experiments were carried out as previously described [25]. In brief,
683 isolated nuclei were digested with MNase to mono-nucleosomes. Paired-end
684 sequencing libraries were prepared (Illumina). Paired reads (50 nt) were mapped to the
685 reference genome (SacCer2) using Bowtie-2 [133-135]. For analysis of nucleosome
686 occupancy (coverage) at tDNAs, both across the genome and on chromosome III,
687 tDNAs were aligned on their start sites or at the deletion points. Data sets were
688 normalized to their genomic average, set at 1, using only DNA fragments in the 120 to
689 180 bp range. In one experiment, mono-nucleosomal DNA was gel-purified, but not in
690 the replicate, in which short fragments (< 120 bp) derived from digestion of the TFIIB-
691 TFIIC complex at tDNAs (Nagarajavel 2013) were observed. The MNase-seq data are
692 available at the GEO database:

693 (GSE98304 [https://www.ncbi.nlm.nih.gov/geo/query/acc.cgi?token=wnynwaoqvntfmb&](https://www.ncbi.nlm.nih.gov/geo/query/acc.cgi?token=wnynwaoqvntfmb&acc=GSE98304)
694 [acc=GSE98304](https://www.ncbi.nlm.nih.gov/geo/query/acc.cgi?token=wnynwaoqvntfmb&acc=GSE98304))

695 **ChIP-Seq and RNA-Seq**

696 Chromatin immunoprecipitation reactions were performed essentially as described
697 above but elution of the precipitated DNA from Protein A/G beads was carried out with
698 two successive washes in 175ul of 0.1M NaHCO₃/1% SDS. 50ul of each input sample
699 was diluted to 350ul with the elution buffer. NaCl was added to a final concentration of

700 0.2M and cross-links were reversed with an overnight incubation at 65C in a
701 Thermomixer. All samples were treated with 60ug of RNAase A (Sigma) at 37C for 60'
702 followed by a Proteinase K (Roche) treatment at 50C for 60'. DNA was purified with a
703 successive phenol chloroform and chloroform extraction followed by precipitation with 2
704 volumes of ethanol and 50ug of glycogen (Roche).

705 The ChIP and Input DNA was spun, washed with 70% ethanol and re-suspended in
706 deionized water. DNA quantitation was performed using a Qubit dsDNA HS Assay kit
707 prior to confirmation by qPCR.

708 Libraries for ChIP-Seq were prepared at the Functional Genomics Laboratory, UC
709 Berkeley and sequenced on an Illumina HiSeq4000 at the Vincent J Coates Laboratory
710 at UC Berkeley.

711 For RNA-Seq, yeast strains JRY2334 and JKY690 were grown in duplicate in 50ml YPD
712 to a cell density of $6-7 \times 10^6$ cells/ml, spun, washed in 25ml PBS, divided into 4 aliquots
713 per culture and transferred to 1.5ml microfuge tubes. Cell pellets were flash frozen in
714 liquid N₂ and transferred to -70C. RNA, library preparation and sequencing for RNA-
715 Seq were performed by ACGT Inc. Wheeling, IL.

716 Transcript abundances were estimated using Kallisto [136]. Differential analysis of gene
717 expression data was performed using the R package Sleuth [137]. Likelihood ratio test
718 and Wald test were used to identify the differentially expressed genes (false discovery
719 rate adjusted p-value (or q-value) < 0.05 in both tests). Since the likelihood ratio test
720 does not produce any metric equivalent to the fold change, we used the Wald test to
721 generates the beta statistic, which approximates to the log₂ fold change in expression
722 between the two conditions.

723 Sequence data have been deposited in the GEO database.

724 <https://www.ncbi.nlm.nih.gov/geo/query/acc.cgi?token=krihsykczdmbpox&acc=GSE106>

725 [250](#)

726 **ChIP**

727 ChIP-qPCR experiments on all Brn1 and Scc2/4 were performed as previously
728 described [20, 35]. In brief, yeast cells of a strain of interest were inoculated and grown
729 overnight in 300 ml of YPD media to an OD of 1-2. These cells were then fixed in 1%
730 formaldehyde for a duration of 2 hours at room temperature. The reaction was then
731 quenched with glycine, and the cells were spun down and washed in 1X PBS. The
732 cross linked cells were then flash frozen in dry ice and stored at -70°C. In preparation
733 for IP, the cells were thawed on ice, broken apart by bead beating, and sonicated to
734 achieve a desired chromatin size of ~300 bp. Once the size of the chromatin was
735 checked, cell debris was cleared from the sample by high-speed centrifugation. The
736 cross linked, sized chromatin was split into 2 samples and IP's were done overnight in
737 the presence of both an antibody to the protein of interest as well as pre-blocked A/G-
738 Sepharose beads at 4°C. 50 µl of input chromatin was also taken from each IP sample
739 prior to addition of the antibody. Chromatin elution was done using 10% Chelex 100
740 (Bio-Rad) along with proteinase K treatment. After elution, both input and IP DNA were
741 quantitated via a Picogreen fluorescent quantification assay (Invitrogen). For each
742 qPCR reaction, input DNA was run in triplicate and IP DNA was run in duplicate. An
743 equal amount of input and IP DNA was used in each individual reaction. The
744 enrichment for a given probe was then calculated as IP/Input, and was further
745 normalized to the OCA4 locus. The results of each ChIP-qPCR are comprised from two

746 independent crosslinks per strain assayed, and for each crosslink two independent IPs
747 were done.

748 **Mean Squared Distance Analysis**

749 Mean-squared distance analysis was carried out as previously described [68, 138, 139].

750 In brief, we built strains that contained a 64x lacO array at specific points along
751 chromosome III. We then integrated a cassette containing an spc29-RFP fusion protein
752 elsewhere in the genome. This protein is an essential kinetochore protein, and
753 therefore serves as a marker for the spindle pole body. The spindle pole body served
754 as a fixed point to which we could measure the movement of our GFP tagged loci in 3D
755 space over a period of 10 minutes. Z-stack images of the cells were taken every 30
756 seconds during the time-lapse, and the data are used to calculate the radius of
757 constraint using the equation: $\langle (X_t - X_{t+\Delta t})^2 \rangle$. MSD curves were generated for each
758 locus in both the WT and tDNA delete strain. The MSD curves were used to calculate
759 the radius of constraint (Rc) for each locus. This analysis was performed in no less than
760 35 cells per genotype assayed. The data were plotted in "NotBoxPlots" (source code
761 obtained from <https://github.com/raacampbell/notBoxPlot>)

762 **HML-HMR Colocalization analysis**

763 Distance assays between *HML* and *HMR* was performed as previously described [20].
764 Fluorescence microscopy was performed on live yeast cells after growing the cells in
765 YMD with Leucine, uracil, tryptophan, lysine, adenine and histidine. Cells were grown to
766 an Od A600 of approximately 0.6. Cells were washed in YMD, placed on YMD-agar
767 patches on slides, and imaged. Microscopy was performed using an Olympus xi70
768 inverted wide-field microscope with DeltaVision precision stage using a Coolsnap HQ2

769 camera and a 100x/1.4 oil objective. The 20 image stacks for each image were acquired
770 with a step size of 200nm using the appropriate wavelength for CFP, YFP, GFP or
771 mCherry. The acquisition software used was softWoRx3.7.1. The images were cropped
772 using Adobe Photoshop. For the distance analysis between *HML* and *HMR*, the
773 distance between the yellow and cyan dots were calculated in nanometers using the
774 “measure” tool in three dimensions. The measured distances were loaded into R
775 software (www.r-project.org) and the data were plotted as a box plot. The box includes
776 the middle 50% of the data with the line in the box being the median value. The data
777 presented are the sum of at least two independent strains.

778 **Single Cell Expression Analysis**

779 Single cell expression analysis was performed as previously described [93]. Briefly,
780 cells were grown in YPD at 30C and placed in a microfluidics device. Time-lapse photos
781 of growing cells were recorded using an Axio Observer Z1 microscope using a 40x
782 objective. The ECYP and EYFP fluorescence intensities were normalized to the highest
783 level of fluorescence observed and the Euchromatic mCherry signal.

784 **Micro-C**

785 Micro-C was performed as previously described [71]. The detailed method have been
786 described [72]. In brief, this technique provides nucleosome level resolution of all of the
787 interactions occurring across the genome by using MNase digestion in lieu of a
788 restriction enzyme as in traditional Hi-C techniques. The interactome data were
789 deposited in the GEO database GSE98543

790 (<https://www.ncbi.nlm.nih.gov/geo/query/acc.cgi?acc=GSE98543>)

791

792 **Antibodies**793 Antibodies used in ChIP were as follows; Scc2-Myc: anti-myc 9E10 (Abcam) = 5 μ l,794 Brn1-HA: anti-HA HA.11 (Covance) = 5 μ l.

795

796 **Figure Legends:**

797 **Figure 1) Drug sensitivity of wild type and tDNA delete strains**

798 Ten-fold serial dilutions of cells starting at 10^7 cells were spotted on YPD plates with
799 varying concentrations of various drugs and allowed to grow for between 2 and 5 days.

800 **Figure 2) Deletion of tDNAs leads to local changes in chromatin structure**

801 A) Comparison of nucleosome occupancy at 265 tDNAs on all of the yeast
802 chromosomes except chromosome III. The tDNAs were aligned with respect to their
803 transcription start sites (TSS set at 0). WT (black) tDNA delete (red).

804 B) Analysis of the nucleosome occupancy at tDNAs on chromosome III in the wild
805 type and tDNA delete strain.

806 C) Comparison of global nucleosome phasing on chromosome III in wild type (blue
807 line) and tDNA delete (red line) cells: average nucleosome dyad positions on 106 RNA
808 Pol II-transcribed genes on chromosome III. These genes cover most of chromosome
809 III. The genes were aligned with respect to their transcription start sites (TSS set at 0).
810 The average nucleosome dyad density is set at 1.

811 D) MNase-seq data for wild type and tDNA delete (normalized to the genomic
812 average (= 1)). Coverage plots are shown using all DNA fragments in the 120 to 180 bp
813 range. The reference point (0) is the nucleotide marking the 5'-end of the deletion on
814 chromosome III. Upstream of the deletion point at 0, the DNA sequence is the same in
815 wild type and the tDNA delete chromosome III. Downstream of the deletion point, the
816 DNA sequences are different. The black arrow shows the location and orientation of the

817 tDNA in wild type chromosome III. Meaningful plots cannot be made for two tDNAs
818 (tP(AGG)C and tS(CGA)C), because they were moved to another chromosome. Two
819 other tDNAs (tM(CAU)C and tK(CUU)C) are present in S288C strains but are naturally
820 absent in W-303 strains, including the strains used here. The wild type profile is in
821 orange and the tDNA delete profile is in blue.

822 **Figure 3) Scc2 binding along chromosome III in the wild type and tDNA delete**
823 **strain**

824 ChIP-seq mapping of Myc-Scc2. The top panels show the distribution of Scc2 at
825 tDNAs on chromosome III in wild type cells (left) and tDNA delete strains (right). Bottom
826 panels show the distribution of Scc2 at 265 tDNAs on all chromosomes except
827 chromosome III in the wild type (left) and the tDNA delete strain (right).

828 **Figure 4) Scc2 and Brn1 binding at tDNAs on chromosome III**

829 A) ChIP-qPCR mapping of Myc-Scc2. The data show the distribution of Scc2 at
830 specific sites along chromosome III in the wild type and tDNA delete strain. The data
831 are the results of two independent crosslinks from which four IP's were performed. For
832 each amplicon, the fold enrichment compared to input was first calculated and the data
833 were then normalized to the *OCA4* locus. An unpaired t-test assuming unequal SD was
834 used to test for significance of differences between the wild type and tDNA delete strain.

835 B) ChIP-qPCR mapping of HA-Brn1, condensin. Fold enrichment and statistical
836 significance was calculated in the same way as for the Scc2 ChIP and normalized to the
837 *OCA4* locus.

838 **Figure 5) Effect of tDNA deletion on chromosome III mobility**

839 Mean square displacement analysis of seven loci along chromosome III in wild type
840 and tDNA delete strains are shown. Box plots represent the data obtained from the
841 MSD experiments. Components of the boxplot are as follows; red line represents the
842 mean, pink bar is the 95% confidence interval, purple bar is the standard deviation, and
843 the grey dots represent individual values obtained from each cell analyzed. The green
844 arrowheads beneath the chromosome III schematic show the locations of the loci
845 assayed. The radius of constraint (R_c) measurement was calculated from MSD graphs
846 that were generated over the course of a 10-minute time-lapse movie. These
847 experiments are the result of time-lapse images taken from at least 35 cells per locus
848 assayed. A t-test was used to determine significance of differences observed between
849 the wild type and tDNA delete strain for each loci.

850 **Figure 6) Micro-C Interaction plots of chromosome III.**

851 A) A snapshot of chromosome IX at 2.5kb resolution and 1kb resolution. The wild
852 type and tDNA delete mutant is shown in the top and bottom of the contact matrix
853 respectively.

854 The lower panel is a view of a segment at 100bp resolution and the insulation score
855 are plotted above the contact matrix. The insulation score is the value obtained by
856 calculating the number of contacts within a 10kbx10kb-sliding window using the 1kb
857 resolution contact matrix. The local minima identify boundaries, which help demarcate
858 CIDs.

859 B) A scatter plot of the insulation scores showing that there is no change in insulation
860 strength between the wild type and tDNA delete strain.

861 C) The interaction decay curve for chromosome III showing that there is no significant
862 changes between the wild type and tDNA delete strain.

863 D) A 4C-type contact graph using a region immediately adjacent to the deleted tRNA
864 gene. The 1-D contact matrix at 5kb resolution was plotted. The Y-axis is the Log2 ratio
865 of differential contacts between the wild type and tDNA delete strain.

866 **Figure 7) Micro-C analysis of the centromeres**

867 A) Contact map of chromosome III for the wild type and tDNA delete strain
868 normalized by distance (obs/exp).

869 B) Differential contact maps were generated by dividing the tDNA matrix by the wild
870 type matrix. Increased contacts in the tDNA delete strain are shown in red and reduced
871 contacts in the tDNA delete strain compared to the wild type strain are shown in blue.

872 C) The graphs are a quantification of *CEN-CEN* interactions. The graph examines the
873 interaction of *CEN16* with all other centromeres. The x-axis is the interaction counts of a
874 50 kb segment centered on each centromere (in parts per million).

875 D) The graph examines the interaction of *CEN3* with all other centromeres. The x-
876 axis is the interaction counts of a 50 kb segment centered on each centromere (in parts
877 per million). The increase in the CEN3-CEN interactions in the tDNA deletion strain was
878 significantly higher ($p=1.22 \times 10^{-14}$) compared to values of all CEN16-CEN interactions

879 (excluding CEN16-CEN3).

880 **Figure 8) Long-Range *HML-HMR* association**

881 A) Deletion of tDNAs on chromosome III leads to a change in *HML-HMR* interaction
882 as measured by Micro-C. Heat maps display the interaction profile between segments
883 on chromosome III that include *HML* and *HMR* (obtained from the Micro-C data).
884 Increased interactions are denoted by red and decreased interactions are denoted by
885 blue. The data are displayed in a log2 format. The x and y axes denote the region of the
886 chromosome displayed on each axis of the heat map.

887 B) Deletion of tDNA t0 leads to perturbation of *HML-HMR* long-range association.
888 The violin plots show data of the distances between *HML::TetR-YFP* and *HMR::CFP-*
889 *LacI* foci in asynchronously growing strains. Mann-Whitney U-Test were performed to
890 determine statistical significance between wild type and the various mutants. Wild type
891 (n=305), *sir4Δ* (n=134) ($p=6.7 \times 10^{-16}$), tDNA t0Δ (n=317) ($p=3.1 \times 10^{-14}$) or t0Δ:NL1 (n=330)
892 ($p=2.2 \times 10^{-16}$) strains. The dark line in the middle represents the median distance. The
893 data for *sir4Δ* are shown as a control and are the same as those in [20].

894 C) Replication–repair proteins are necessary for *HML-HMR* interactions:
895 Violin plots of the distance between TetR-YFP and CFP-LacI foci in a given wild type
896 or mutant strain are shown. *rrm3Δ* (n=208) ($p=4.8 \times 10^{-12}$), *dpb3Δ* (n=134) ($p=1.7 \times 10^{-10}$)
897 *top1Δ* (n=139) ($p=4.2 \times 10^{-12}$) *scc2D730V* (n=188) ($p=1.9 \times 10^{-14}$). The data for the
898 *scc2D730V* allele are simply shown as a control and are the same as those in [20].

899 **Figure 9) Silencing of reporter genes at *HML* and *HMR***

900 A) tDNAs on chromosome III modulate silencing of reporter genes at *HML* and *HMR*.
901 Representative lineage trees of the different strains that were analyzed are shown. Wild
902 type refers to a strain containing all tDNAs on chromosome III. tDNA delete refers to a
903 strain lacking any tDNAs on chromosome III. The expression of *HML::EYFP* or
904 *HMR::ECFP* in each generation of cells was monitored, quantitated and is indicated by
905 the presence of their respective colors in the cells of the tree.

906 B) Deletion of tDNAs on chromosome III leads to a change in the maintenance of
907 silencing at *HML* and *HMR*. The graphs quantify the changes in expression state of
908 *HML::EYFP* and *HMR::ECFP* between generations in the different genotypes studied.
909 Expressed to repressed transitions identify reporters that were expressed in one
910 generation but not expressed in the next. Repressed to expressed transitions represent
911 reporter genes that were not expressed in one generation but expressed in the next.

912 **Table1**

913 Genes whose mRNA levels changed in the tDNA delete strain compared to the wild
914 type along with statistical analysis of the differences in expression levels.

915 **Table2**

916 Strain list with genotypes

917 **Table3**

918 Sequences of PCR primers used in this study

919 **Table4**

920 Statistical analysis of differences in expression of HML::EYFP and HMR::ECFP in the
921 wild type and tDNA delete strains.
922
923
924
925

926 **References**

927

- 928 1. Taddei, A., H. Schober, and S.M. Gasser, *The budding yeast nucleus*. Cold
929 Spring Harb Perspect Biol, 2010. **2**(8): p. a000612.
- 930 2. Zimmer, C. and E. Fabre, *Principles of chromosomal organization: lessons from*
931 *yeast*. J Cell Biol, 2011. **192**(5): p. 723-33.
- 932 3. Palladino, F., T. Laroche, E. Gilson, L. Pillus, and S.M. Gasser, *The positioning*
933 *of yeast telomeres depends on SIR3, SIR4, and the integrity of the nuclear*
934 *membrane*. Cold Spring Harb Symp Quant Biol, 1993. **58**: p. 733-46.
- 935 4. Ruben, G.J., J.G. Kirkland, T. Macdonough, M. Chen, R.N. Dubey, M.R.
936 Gartenberg, and R.T. Kamakaka, *Nucleoporin Mediated Nuclear Positioning and*
937 *Silencing of HMR*. PLoS One, 2011. **6**(7): p. e21923.
- 938 5. Fabre, E. and M. Spichal, *Subnuclear Architecture of telomeres and*
939 *subtelomeres in yeast*, in *SubTelomeres*, E.J. Louis and M.M. Becker, Editors.
940 2014, Springer. p. 13-37.
- 941 6. Oakes, M., J.P. Aris, J.S. Brockenbrough, H. Wai, L. Vu, and M. Nomura,
942 *Mutational analysis of the structure and localization of the nucleolus in the yeast*
943 *Saccharomyces cerevisiae*. J Cell Biol, 1998. **143**(1): p. 23-34.
- 944 7. Jin, Q.W., J. Fuchs, and J. Loidl, *Centromere clustering is a major determinant of*
945 *yeast interphase nuclear organization*. J Cell Sci, 2000. **113** (Pt 11): p. 1903-12.
- 946 8. Therizols, P., T. Duong, B. Dujon, C. Zimmer, and E. Fabre, *Chromosome arm*
947 *length and nuclear constraints determine the dynamic relationship of yeast*
948 *subtelomeres*. Proc Natl Acad Sci U S A, 2010. **107**(5): p. 2025-30.
- 949 9. Tjong, H., K. Gong, L. Chen, and F. Alber, *Physical tethering and volume*
950 *exclusion determine higher-order genome organization in budding yeast*.
951 Genome Res, 2012. **22**(7): p. 1295-305.
- 952 10. Duan, Z., M. Andronescu, K. Schutz, S. McIlwain, Y.J. Kim, C. Lee, J. Shendure,
953 S. Fields, C.A. Blau, and W.S. Noble, *A three-dimensional model of the yeast*
954 *genome*. Nature, 2010. **465**(7296): p. 363-7.
- 955 11. Palladino, F., T. Laroche, E. Gilson, A. Axelrod, L. Pillus, and S.M. Gasser, *SIR3*
956 *and SIR4 proteins are required for the positioning and integrity of yeast*
957 *telomeres*. Cell, 1993. **75**: p. 543-555.
- 958 12. Andrulis, E.D., D.C. Zappulla, A. Ansari, S. Perrod, C.V. Laiosa, M.R.
959 Gartenberg, and R. Sternglanz, *Esc1, a nuclear periphery protein required for*
960 *Sir4-based plasmid anchoring and partitioning*. Mol Cell Biol, 2002. **22**(23): p.
961 8292-301.
- 962 13. Taddei, A., F. Hediger, F.R. Neumann, C. Bauer, and S.M. Gasser, *Separation of*
963 *silencing from perinuclear anchoring functions in yeast Ku80, Sir4 and Esc1*
964 *proteins*. Embo J, 2004. **23**(6): p. 1301-12.
- 965 14. Taddei, A., M.R. Gartenberg, F.R. Neumann, F. Hediger, and S.M. Gasser,
966 *Multiple pathways tether telomeres and silent chromatin at the nuclear periphery:*
967 *functional implications for sir-mediated repression*. Novartis Found Symp, 2005.
968 **264**: p. 140-56; discussion 156-65, 227-30.

15. Bupp, J.M., A.E. Martin, E.S. Stensrud, and S.L. Jaspersen, *Telomere anchoring at the nuclear periphery requires the budding yeast Sad1-UNC-84 domain protein Mps3*. J Cell Biol, 2007. **179**(5): p. 845-54.
16. Mekhail, K., J. Seebacher, S.P. Gygi, and D. Moazed, *Role for perinuclear chromosome tethering in maintenance of genome stability*. Nature, 2008. **456**(7222): p. 667-70.
17. Klein, F., T. Laroche, M.E. Cardenas, J.F. Hofmann, D. Schweizer, and S.M. Gasser, *Localization of RAP1 and topoisomerase II in nuclei and meiotic chromosomes of yeast*. J Cell Biol, 1992. **117**(5): p. 935-48.
18. Taddei, A., G. Van Houwe, F. Hediger, V. Kalck, F. Cubizolles, H. Schober, and S.M. Gasser, *Nuclear pore association confers optimal expression levels for an inducible yeast gene*. Nature, 2006. **441**(7094): p. 774-8.
19. Kirkland, J., M.R. Peterson, C.B. Still, L. Brueggemann, N. Dhillon, and R. Kamakaka, *Heterochromatin formation via recruitment of DNA repair proteins*. Molecular Biology of Cell, 2015.
20. Kirkland, J.G. and R.T. Kamakaka, *Long-range heterochromatin association is mediated by silencing and double-strand DNA break repair proteins*. J Cell Biol, 2013. **201**(6): p. 809-26.
21. Dieci, G., G. Fiorino, M. Castelnovo, M. Teichmann, and A. Pagano, *The expanding RNA polymerase III transcriptome*. Trends Genet, 2007.
22. Oki, M. and R.T. Kamakaka, *Barrier Function at HMR*. Mol Cell, 2005. **19**(5): p. 707-16.
23. Weiner, A., A. Hughes, M. Yassour, O.J. Rando, and N. Friedman, *High-resolution nucleosome mapping reveals transcription-dependent promoter packaging*. Genome Res, 2010. **20**(1): p. 90-100.
24. Yuan, G.C., Y.J. Liu, M.F. Dion, M.D. Slack, L.F. Wu, S.J. Altschuler, and O.J. Rando, *Genome-scale identification of nucleosome positions in S. cerevisiae*. Science, 2005. **309**(5734): p. 626-30.
25. Cole, H.A., B.H. Howard, and D.J. Clark, *Genome-wide mapping of nucleosomes in yeast using paired-end sequencing*. Methods Enzymol, 2012. **513**: p. 145-68.
26. Geiduschek, E.P. and G.A. Kassavetis, *The RNA polymerase III transcription apparatus*. J Mol Biol, 2001. **310**(1): p. 1-26.
27. Schramm, L. and N. Hernandez, *Recruitment of RNA polymerase III to its target promoters*. Genes Dev, 2002. **16**(20): p. 2593-620.
28. Glynn, E.F., P.C. Megee, H.G. Yu, C. Mistrot, E. Unal, D.E. Koshland, J.L. DeRisi, and J.L. Gerton, *Genome-wide mapping of the cohesin complex in the yeast Saccharomyces cerevisiae*. PLoS Biol, 2004. **2**(9): p. E259.
29. D'Ambrosio, C., C.K. Schmidt, Y. Katou, G. Kelly, T. Itoh, K. Shirahige, and F. Uhlmann, *Identification of cis-acting sites for condensin loading onto budding yeast chromosomes*. Genes Dev, 2008. **22**(16): p. 2215-27.
30. Haeusler, R.A., M. Pratt-Hyatt, P.D. Good, T.A. Gipson, and D.R. Engelke, *Clustering of yeast tRNA genes is mediated by specific association of condensin with tRNA gene transcription complexes*. Genes Dev, 2008. **22**(16): p. 2204-14.
31. Lopez-Serra, L., G. Kelly, H. Patel, A. Stewart, and F. Uhlmann, *The Scc2-Scc4 complex acts in sister chromatid cohesion and transcriptional regulation by maintaining nucleosome-free regions*. Nat Genet, 2014. **46**(10): p. 1147-51.

- 1015 32. Kogut, I., J. Wang, V. Guacci, R.K. Mistry, and P.C. Megee, *The Scc2/Scc4*
1016 *cohesin loader determines the distribution of cohesin on budding yeast*
1017 *chromosomes*. Genes Dev, 2009. **23**(19): p. 2345-57.
- 1018 33. Bausch, C., S. Noone, J.M. Henry, K. Gaudenz, B. Sanderson, C. Seidel, and
1019 J.L. Gerton, *Transcription alters chromosomal locations of cohesin in*
1020 *Saccharomyces cerevisiae*. Mol Cell Biol, 2007. **27**(24): p. 8522-32.
- 1021 34. Huang, J. and B.C. Laurent, *A Role for the RSC chromatin remodeler in*
1022 *regulating cohesion of sister chromatid arms*. Cell Cycle, 2004. **3**(8): p. 973-5.
- 1023 35. Dhillon, N., J. Raab, J. Guzzo, S.J. Szyjka, S. Gangadharan, O.M. Aparicio, B.
1024 Andrews, and R.T. Kamakaka, *DNA polymerase epsilon, acetylases and*
1025 *remodellers cooperate to form a specialized chromatin structure at a tRNA*
1026 *insulator*. Embo J, 2009. **28**(17): p. 2583-600.
- 1027 36. Frenkel, F.E., M.B. Chaley, E.V. Korotkov, and K.G. Skryabin, *Evolution of tRNA-*
1028 *like sequences and genome variability*. Gene, 2004. **335**: p. 57-71.
- 1029 37. Goodenbour, J.M. and T. Pan, *Diversity of tRNA genes in eukaryotes*. Nucleic
1030 Acids Res, 2006. **34**(21): p. 6137-46.
- 1031 38. Withers, M., L. Wernisch, and M. dos Reis, *Archaeology and evolution of transfer*
1032 *RNA genes in the Escherichia coli genome*. Rna, 2006. **12**(6): p. 933-42.
- 1033 39. Raab, J.R., J. Chiu, J. Zhu, S. Katzman, S. Kurukuti, P.A. Wade, D. Haussler,
1034 and R.T. Kamakaka, *Human tRNA genes function as chromatin insulators*.
1035 EMBO J, 2012. **31**(2): p. 330-50.
- 1036 40. Wang, J., V.V. Lunyak, and I.K. Jordan, *Genome-wide prediction and analysis of*
1037 *human chromatin boundary elements*. Nucleic Acids Res, 2012. **40**(2): p. 511-29.
- 1038 41. Van Bortle, K. and V.G. Corces, *tDNA insulators and the emerging role of TFIIIC*
1039 *in genome organization*. Transcription, 2012. **3**(6): p. 277-84.
- 1040 42. Kirkland, J.G., J.R. Raab, and R.T. Kamakaka, *TFIIIC bound DNA elements in*
1041 *nuclear organization and insulation*. Biochim Biophys Acta, 2013. **1829**(3-4): p.
1042 418-24.
- 1043 43. Donze, D., C.R. Adams, J. Rine, and R.T. Kamakaka, *The boundaries of the*
1044 *silenced HMR domain in Saccharomyces cerevisiae*. Genes Dev, 1999. **13**(6): p.
1045 698-708.
- 1046 44. Biswas, M., N. Maqani, R. Rai, S.P. Kumaran, K.R. Iyer, E. Sendinc, J.S. Smith,
1047 and S. Laloraya, *Limiting the extent of the RDN1 heterochromatin domain by a*
1048 *silencing barrier and Sir2 protein levels in Saccharomyces cerevisiae*. Mol Cell
1049 Biol, 2009. **29**(10): p. 2889-98.
- 1050 45. Korde, A., J.M. Rosselot, and D. Donze, *Intergenic Transcriptional Interference Is*
1051 *Blocked by RNA Polymerase III Transcription Factor TFIIIB in Saccharomyces*
1052 *cerevisiae*. Genetics, 2013. **196**(2): p. 427-38.
- 1053 46. Simms, T.A., E.C. Miller, N.P. Buisson, N. Jambunathan, and D. Donze, *The*
1054 *Saccharomyces cerevisiae TRT2 tRNAThr gene upstream of STE6 is a barrier to*
1055 *repression in MATalpha cells and exerts a potential tRNA position effect in MATa*
1056 *cells*. Nucleic Acids Res, 2004. **32**(17): p. 5206-13.
- 1057 47. Simms, T.A., S.L. Dugas, J.C. Gremillion, M.E. Ibos, M.N. Dandurand, T.T.
1058 Toliver, D.J. Edwards, and D. Donze, *TFIIIC binding sites function as both*
1059 *heterochromatin barriers and chromatin insulators in Saccharomyces cerevisiae*.
1060 Eukaryot Cell, 2008. **7**(12): p. 2078-86.

- 1061 48. Van Bortle, K., M.H. Nichols, L. Li, C.T. Ong, N. Takenaka, Z.S. Qin, and V.G.
1062 Corces, *Insulator function and topological domain border strength scale with*
1063 *architectural protein occupancy*. Genome Biol, 2014. **15**(6): p. R82.
- 1064 49. Ebersole, T., J.H. Kim, A. Samoshkin, N. Kouprina, A. Pavlicek, R.J. White, and
1065 V. Larionov, *tRNA genes protect a reporter gene from epigenetic silencing in*
1066 *mouse cells*. Cell Cycle, 2011. **10**(16): p. 2779-91.
- 1067 50. Dixon, J.R., S. Selvaraj, F. Yue, A. Kim, Y. Li, Y. Shen, M. Hu, J.S. Liu, and B.
1068 Ren, *Topological domains in mammalian genomes identified by analysis of*
1069 *chromatin interactions*. Nature, 2012. **485**(7398): p. 376-80.
- 1070 51. Good, P.D., A. Kendall, J. Ignatz-Hoover, E.L. Miller, D.A. Pai, S.R. Rivera, B.
1071 Carrick, and D.R. Engelke, *Silencing near tRNA genes is nucleosome-mediated*
1072 *and distinct from boundary element function*. Gene, 2013. **526**(1): p. 7-15.
- 1073 52. Thompson, M., R.A. Haeusler, P.D. Good, and D.R. Engelke, *Nucleolar*
1074 *clustering of dispersed tRNA genes*. Science, 2003. **302**(5649): p. 1399-401.
- 1075 53. Pombo, A., D.A. Jackson, M. Hollinshead, Z. Wang, R.G. Roeder, and P.R.
1076 Cook, *Regional specialization in human nuclei: visualization of discrete sites of*
1077 *transcription by RNA polymerase III*. Embo J, 1999. **18**(8): p. 2241-53.
- 1078 54. Haeusler, R.A. and D.R. Engelke, *Spatial organization of transcription by RNA*
1079 *polymerase III*. Nucleic Acids Res, 2006. **34**(17): p. 4826-36.
- 1080 55. Iwasaki, O., A. Tanaka, H. Tanizawa, S.I. Grewal, and K. Noma, *Centromeric*
1081 *localization of dispersed Pol III genes in fission yeast*. Mol Biol Cell, 2010. **21**(2):
1082 p. 254-65.
- 1083 56. Schalbetter, S.A., A. Goloborodko, G. Fudenberg, J.M. Belton, C. Miles, M. Yu, J.
1084 Dekker, L. Mirny, and J. Baxter, *SMC complexes differentially compact mitotic*
1085 *chromosomes according to genomic context*. Nat Cell Biol, 2017. **19**(9): p. 1071-
1086 1080.
- 1087 57. Haeusler, R.A. and D.R. Engelke, *Genome organization in three dimensions:*
1088 *thinking outside the line*. Cell Cycle, 2004. **3**(3): p. 273-5.
- 1089 58. Iwasaki, O. and K. Noma, *Global genome organization mediated by RNA*
1090 *polymerase III-transcribed genes in fission yeast*. Gene, 2012. **493**(2): p. 195-
1091 200.
- 1092 59. Ho, C.K. and J. Abelson, *Testing for intron function in the essential*
1093 *Saccharomyces cerevisiae tRNA(SerUCG) gene*. J Mol Biol, 1988. **202**(3): p.
1094 667-72.
- 1095 60. Bloom-Ackermann, Z., S. Navon, H. Gingold, R. Towers, Y. Pilpel, and O.
1096 Dahan, *A comprehensive tRNA deletion library unravels the genetic architecture*
1097 *of the tRNA pool*. PLoS Genet, 2014. **10**(1): p. e1004084.
- 1098 61. Dion, M.F., T. Kaplan, M. Kim, S. Buratowski, N. Friedman, and O.J. Rando,
1099 *Dynamics of replication-independent histone turnover in budding yeast*. Science,
1100 2007. **315**(5817): p. 1405-8.
- 1101 62. Chereji, R.V., J. Ocampo, and D.J. Clark, *MNase-Sensitive Complexes in Yeast:*
1102 *Nucleosomes and Non-histone Barriers*. Mol Cell, 2017. **65**(3): p. 565-577 e3.
- 1103 63. Uhlmann, F., *SMC complexes: from DNA to chromosomes*. Nat Rev Mol Cell
1104 Biol, 2016. **17**(7): p. 399-412.
- 1105 64. Parnell, T.J., J.T. Huff, and B.R. Cairns, *RSC regulates nucleosome positioning*
1106 *at Pol II genes and density at Pol III genes*. Embo J, 2008. **27**(1): p. 100-10.

- 1107 65. Damelin, M., I. Simon, T.I. Moy, B. Wilson, S. Komili, P. Tempst, F.P. Roth, R.A.
1108 Young, B.R. Cairns, and P.A. Silver, *The genome-wide localization of Rsc9, a*
1109 *component of the RSC chromatin-remodeling complex, changes in response to*
1110 *stress*. Mol Cell, 2002. **9**(3): p. 563-73.
- 1111 66. Dion, V., V. Kalck, C. Horigome, B.D. Towbin, and S.M. Gasser, *Increased*
1112 *mobility of double-strand breaks requires Mec1, Rad9 and the homologous*
1113 *recombination machinery*. Nat Cell Biol, 2012.
- 1114 67. Mine-Hattab, J. and R. Rothstein, *Increased chromosome mobility facilitates*
1115 *homology search during recombination*. Nat Cell Biol, 2012.
- 1116 68. Verdaasdonk, J.S., P.A. Vasquez, R.M. Barry, T. Barry, S. Goodwin, M.G.
1117 Forest, and K. Bloom, *Centromere tethering confines chromosome domains*. Mol
1118 Cell, 2013. **52**(6): p. 819-31.
- 1119 69. Albert, B., J. Mathon, A. Shukla, H. Saad, C. Normand, I. Leger-Silvestre, D.
1120 Villa, A. Kamgoue, J. Mozziconacci, H. Wong, C. Zimmer, P. Bhargava, A.
1121 Bancaud, and O. Gadai, *Systematic characterization of the conformation and*
1122 *dynamics of budding yeast chromosome XII*. J Cell Biol, 2013. **202**(2): p. 201-10.
- 1123 70. Noma, K., H.P. Cam, R.J. Maraia, and S.I. Grewal, *A role for TFIIIC transcription*
1124 *factor complex in genome organization*. Cell, 2006. **125**(5): p. 859-72.
- 1125 71. Hsieh, T.H., A. Weiner, B. Lajoie, J. Dekker, N. Friedman, and O.J. Rando,
1126 *Mapping Nucleosome Resolution Chromosome Folding in Yeast by Micro-C*.
1127 Cell, 2015. **162**(1): p. 108-19.
- 1128 72. Hsieh, T.S., G. Fudenberg, A. Goloborodko, and O.J. Rando, *Micro-C XL:*
1129 *assaying chromosome conformation from the nucleosome to the entire genome*.
1130 Nat Methods, 2016. **13**(12): p. 1009-1011.
- 1131 73. Guacci, V., E. Hogan, and D. Koshland, *Centromere position in budding yeast:*
1132 *evidence for anaphase A*. Mol Biol Cell, 1997. **8**(6): p. 957-72.
- 1133 74. Jin, Q., E. Trelles-Sticken, H. Scherthan, and J. Loidl, *Yeast nuclei display*
1134 *prominent centromere clustering that is reduced in nondividing cells and in*
1135 *meiotic prophase*. J Cell Biol, 1998. **141**(1): p. 21-9.
- 1136 75. Dekker, J., K. Rippe, M. Dekker, and N. Kleckner, *Capturing chromosome*
1137 *conformation*. Science, 2002. **295**(5558): p. 1306-11.
- 1138 76. Kumaran, R., S.Y. Yang, and J.Y. Leu, *Characterization of chromosome stability*
1139 *in diploid, polyploid and hybrid yeast cells*. PLoS One, 2013. **8**(7): p. e68094.
- 1140 77. Miele, A., K. Bystricky, and J. Dekker, *Yeast silent mating type loci form*
1141 *heterochromatic clusters through silencer protein-dependent long-range*
1142 *interactions*. PLoS Genet, 2009. **5**(5): p. e1000478.
- 1143 78. Dubarry, M., I. Loiodice, C.L. Chen, C. Thermes, and A. Taddei, *Tight protein-*
1144 *DNA interactions favor gene silencing*. Genes Dev, 2011. **25**(13): p. 1365-70.
- 1145 79. Giorgetti, L. and E. Heard, *Closing the loop: 3C versus DNA FISH*. Genome Biol,
1146 2016. **17**(1): p. 215.
- 1147 80. Fraser, J., I. Williamson, W.A. Bickmore, and J. Dostie, *An Overview of Genome*
1148 *Organization and How We Got There: from FISH to Hi-C*. Microbiol Mol Biol Rev,
1149 2015. **79**(3): p. 347-72.
- 1150 81. Williamson, I., S. Berlivet, R. Eskeland, S. Boyle, R.S. Illingworth, D. Paquette, J.
1151 Dostie, and W.A. Bickmore, *Spatial genome organization: contrasting views from*

- 1152 chromosome conformation capture and fluorescence in situ hybridization. *Genes*
1153 *Dev*, 2014. **28**(24): p. 2778-91.
- 1154 82. Dubey, R.N. and M.R. Gartenberg, *A tDNA establishes cohesion of a*
1155 *neighboring silent chromatin domain*. *Genes Dev*, 2007. **21**(17): p. 2150-60.
- 1156 83. Donze, D. and R.T. Kamakaka, *RNA polymerase III and RNA polymerase II*
1157 *promoter complexes are heterochromatin barriers in Saccharomyces cerevisiae*.
1158 *Embo J*, 2001. **20**(3): p. 520-31.
- 1159 84. Valenzuela, L., N. Dhillon, and R.T. Kamakaka, *Transcription independent*
1160 *insulation at TFIIIC-dependent insulators*. *Genetics*, 2009. **183**(1): p. 131-48.
- 1161 85. Dilworth, D.J., A.J. Tackett, R.S. Rogers, E.C. Yi, R.H. Christmas, J.J. Smith,
1162 A.F. Siegel, B.T. Chait, R.W. Wozniak, and J.D. Aitchison, *The mobile*
1163 *nucleoporin Nup2p and chromatin-bound Prp20p function in endogenous NPC-*
1164 *mediated transcriptional control*. *J Cell Biol*, 2005. **171**(6): p. 955-65.
- 1165 86. Deshpande, A.M. and C.S. Newlon, *DNA replication fork pause sites dependent*
1166 *on transcription*. *Science*, 1996. **272**(5264): p. 1030-3.
- 1167 87. Azvolinsky, A., P.G. Giresi, J.D. Lieb, and V.A. Zakian, *Highly transcribed RNA*
1168 *polymerase II genes are impediments to replication fork progression in*
1169 *Saccharomyces cerevisiae*. *Mol Cell*, 2009. **34**(6): p. 722-34.
- 1170 88. Achar, Y.J. and M. Foiani, *Coordinating Replication with Transcription*. *Adv Exp*
1171 *Med Biol*, 2017. **1042**: p. 455-487.
- 1172 89. Szilard, R.K., P.E. Jacques, L. Laramée, B. Cheng, S. Galicia, A.R. Bataille, M.
1173 Yeung, M. Mendez, M. Bergeron, F. Robert, and D. Durocher, *Systematic*
1174 *identification of fragile sites via genome-wide location analysis of gamma-H2AX*.
1175 *Nat Struct Mol Biol*, 2010. **17**(3): p. 299-305.
- 1176 90. Lengronne, A., Y. Katou, S. Mori, S. Yokobayashi, G.P. Kelly, T. Itoh, Y.
1177 Watanabe, K. Shirahige, and F. Uhlmann, *Cohesin relocation from sites of*
1178 *chromosomal loading to places of convergent transcription*. *Nature*, 2004.
1179 **430**(6999): p. 573-8.
- 1180 91. Ivessa, A.S., B.A. Lenzmeier, J.B. Bessler, L.K. Goudsouzian, S.L.
1181 Schnakenberg, and V.A. Zakian, *The Saccharomyces cerevisiae helicase Rrm3p*
1182 *facilitates replication past nonhistone protein-DNA complexes*. *Mol Cell*, 2003.
1183 **12**(6): p. 1525-36.
- 1184 92. Azvolinsky, A., S. Dunaway, J.Z. Torres, J.B. Bessler, and V.A. Zakian, *The S.*
1185 *cerevisiae Rrm3p DNA helicase moves with the replication fork and affects*
1186 *replication of all yeast chromosomes*. *Genes Dev*, 2006. **20**(22): p. 3104-16.
- 1187 93. Mano, Y., T.J. Kobayashi, J. Nakayama, H. Uchida, and M. Oki, *Single cell*
1188 *visualization of yeast gene expression shows correlation of epigenetic switching*
1189 *between multiple heterochromatic regions through multiple generations*. *PLoS*
1190 *Biol*, 2013. **11**(7): p. e1001601.
- 1191 94. Valenzuela, L., S. Gangadharan, and R.T. Kamakaka, *Analyses of SUM1-1-*
1192 *mediated long-range repression*. *Genetics*, 2006. **172**(1): p. 99-112.
- 1193 95. Valenzuela, L., N. Dhillon, R.N. Dubey, M.R. Gartenberg, and R.T. Kamakaka,
1194 *Long-range communication between the silencers of HMR*. *Mol Cell Biol*, 2008.
1195 **28**(6): p. 1924-35.

- 1196 96. Fu, Y., M. Sinha, C.L. Peterson, and Z. Weng, *The insulator binding protein*
1197 *CTCF positions 20 nucleosomes around its binding sites across the human*
1198 *genome*. PLoS Genet, 2008. **4**(7): p. e1000138.
- 1199 97. Nagarajavel, V., J.R. Iben, B.H. Howard, R.J. Maraia, and D.J. Clark, *Global*
1200 *'bootprinting' reveals the elastic architecture of the yeast TFIIB-TFIIC*
1201 *transcription complex in vivo*. Nucleic Acids Res, 2013. **41**(17): p. 8135-43.
- 1202 98. Roberts, D.N., A.J. Stewart, J.T. Huff, and B.R. Cairns, *The RNA polymerase III*
1203 *transcriptome revealed by genome-wide localization and activity-occupancy*
1204 *relationships*. Proc Natl Acad Sci U S A, 2003. **100**(25): p. 14695-700.
- 1205 99. Moqtaderi, Z. and K. Struhl, *Genome-wide occupancy profile of the RNA*
1206 *polymerase III machinery in Saccharomyces cerevisiae reveals loci with*
1207 *incomplete transcription complexes*. Mol Cell Biol, 2004. **24**(10): p. 4118-27.
- 1208 100. Harismendy, O., C.G. Gendrel, P. Soularue, X. Gidrol, A. Sentenac, M. Werner,
1209 and O. Lefebvre, *Genome-wide location of yeast RNA polymerase III*
1210 *transcription machinery*. Embo J, 2003. **22**(18): p. 4738-47.
- 1211 101. Blat, Y. and N. Kleckner, *Cohesins bind to preferential sites along yeast*
1212 *chromosome III, with differential regulation along arms versus the centric region*.
1213 Cell, 1999. **98**(2): p. 249-59.
- 1214 102. Laloraya, S., V. Guacci, and D. Koshland, *Chromosomal addresses of the*
1215 *cohesin component Mcd1p*. J Cell Biol, 2000. **151**(5): p. 1047-56.
- 1216 103. Lindroos, H.B., L. Strom, T. Itoh, Y. Katou, K. Shirahige, and C. Sjogren,
1217 *Chromosomal association of the Smc5/6 complex reveals that it functions in*
1218 *differently regulated pathways*. Mol Cell, 2006. **22**(6): p. 755-67.
- 1219 104. Klein, F., P. Mahr, M. Galova, S.B. Bonomo, C. Michaelis, K. Nairz, and K.
1220 Nasmyth, *A central role for cohesins in sister chromatid cohesion, formation of*
1221 *axial elements, and recombination during yeast meiosis*. Cell, 1999. **98**(1): p. 91-
1222 103.
- 1223 105. Noma, K.I., *The Yeast Genomes in Three Dimensions: Mechanisms and*
1224 *Functions*. Annu Rev Genet, 2017.
- 1225 106. Heidinger-Pauli, J.M., O. Mert, C. Davenport, V. Guacci, and D. Koshland,
1226 *Systematic reduction of cohesin differentially affects chromosome segregation,*
1227 *condensation, and DNA repair*. Curr Biol, 2010. **20**(10): p. 957-63.
- 1228 107. Annaluru, N., H. Muller, L.A. Mitchell, S. Ramalingam, G. Stracquadanio, S.M.
1229 Richardson, J.S. Dymond, Z. Kuang, L.Z. Scheifele, E.M. Cooper, Y. Cai, K.
1230 Zeller, N. Agmon, J.S. Han, M. Hadjithomas, J. Tullman, K. Caravelli, K. Cirelli, Z.
1231 Guo, V. London, A. Yeluru, S. Murugan, K. Kandavelou, N. Agier, G. Fischer, K.
1232 Yang, J.A. Martin, M. Bilgel, P. Bohutski, K.M. Boulter, B.J. Capaldo, J. Chang,
1233 K. Charoen, W.J. Choi, P. Deng, J.E. DiCarlo, J. Doong, J. Dunn, J.I. Feinberg,
1234 C. Fernandez, C.E. Floria, D. Gladowski, P. Hadidi, I. Ishizuka, J. Jabbari, C.Y.
1235 Lau, P.A. Lee, S. Li, D. Lin, M.E. Linder, J. Ling, J. Liu, J. Liu, M. London, H. Ma,
1236 J. Mao, J.E. McDade, A. McMillan, A.M. Moore, W.C. Oh, Y. Ouyang, R. Patel,
1237 M. Paul, L.C. Paulsen, J. Qiu, A. Rhee, M.G. Rubashkin, I.Y. Soh, N.E. Sotuyo,
1238 V. Srinivas, A. Suarez, A. Wong, R. Wong, W.R. Xie, Y. Xu, A.T. Yu, R. Koszul,
1239 J.S. Bader, J.D. Boeke, and S. Chandrasegaran, *Total synthesis of a functional*
1240 *designer eukaryotic chromosome*. Science, 2014. **344**(6179): p. 55-8.

- 1241 108. Mercy, G., J. Mozziconacci, V.F. Scolari, K. Yang, G. Zhao, A. Thierry, Y. Luo,
1242 L.A. Mitchell, M. Shen, Y. Shen, R. Walker, W. Zhang, Y. Wu, Z.X. Xie, Z. Luo, Y.
1243 Cai, J. Dai, H. Yang, Y.J. Yuan, J.D. Boeke, J.S. Bader, H. Muller, and R. Koszul,
1244 *3D organization of synthetic and scrambled chromosomes*. Science, 2017.
1245 **355**(6329).
- 1246 109. Dujon, B., *The yeast genome project: what did we learn?* Trends in Genet., 1996.
1247 **12**(7): p. 263-270.
- 1248 110. Sharp, P.M. and A.T. Lloyd, *Regional base composition variation along yeast*
1249 *chromosome III: evolution of chromosome primary structure*. Nucleic Acids Res,
1250 1993. **21**(2): p. 179-83.
- 1251 111. Dekker, J., *GC- and AT-rich chromatin domains differ in conformation and*
1252 *histone modification status and are differentially modulated by Rpd3p*. Genome
1253 Biol, 2007. **8**(6): p. R116.
- 1254 112. Blat, Y., R.U. Protacio, N. Hunter, and N. Kleckner, *Physical and functional*
1255 *interactions among basic chromosome organizational features govern early steps*
1256 *of meiotic chiasma formation*. Cell, 2002. **111**(6): p. 791-802.
- 1257 113. Raab, J.R. and R.T. Kamakaka, *Insulators and promoters: closer than we think*.
1258 Nat Rev Genet, 2010. **11**(6): p. 439-46.
- 1259 114. Gehlen, L.R., G. Gruenert, M.B. Jones, C.D. Rodley, J. Langowski, and J.M.
1260 O'Sullivan, *Chromosome positioning and the clustering of functionally related loci*
1261 *in yeast is driven by chromosomal interactions*. Nucleus, 2012. **3**(4): p. 370-83.
- 1262 115. Baudat, F. and A. Nicolas, *Clustering of meiotic double-strand breaks on yeast*
1263 *chromosome III*. Proc Natl Acad Sci U S A, 1997. **94**(10): p. 5213-8.
- 1264 116. Gerton, J.L., J. DeRisi, R. Shroff, M. Lichten, P.O. Brown, and T.D. Petes, *Global*
1265 *mapping of meiotic recombination hotspots and coldspots in the yeast*
1266 *Saccharomyces cerevisiae*. Proc Natl Acad Sci U S A, 2000. **97**(21): p. 11383-
1267 90.
- 1268 117. Bystricky, K., P. Heun, L. Gehlen, J. Langowski, and S.M. Gasser, *Long-range*
1269 *compaction and flexibility of interphase chromatin in budding yeast analyzed by*
1270 *high-resolution imaging techniques*. Proc Natl Acad Sci U S A, 2004. **101**(47): p.
1271 16495-500.
- 1272 118. Gartenberg, M.R., F.R. Neumann, T. Laroche, M. Blaszczyk, and S.M. Gasser,
1273 *Sir-mediated repression can occur independently of chromosomal and*
1274 *subnuclear contexts*. Cell, 2004. **119**(7): p. 955-67.
- 1275 119. Taddei, A. and S.M. Gasser, *Multiple pathways for telomere tethering: functional*
1276 *implications of subnuclear position for heterochromatin formation*. Biochim
1277 Biophys Acta, 2004. **1677**(1-3): p. 120-8.
- 1278 120. Schober, H., H. Ferreira, V. Kalck, L.R. Gehlen, and S.M. Gasser, *Yeast*
1279 *telomerase and the SUN domain protein Mps3 anchor telomeres and repress*
1280 *subtelomeric recombination*. Genes Dev, 2009. **23**(8): p. 928-38.
- 1281 121. Snider, C.E., A.D. Stephens, J.G. Kirkland, O. Hamdani, R.T. Kamakaka, and K.
1282 Bloom, *Dyskerin, tRNA genes, and condensin tether pericentric chromatin to the*
1283 *spindle axis in mitosis*. J Cell Biol, 2014. **207**(2): p. 189-99.
- 1284 122. Casolari, J.M., C.R. Brown, S. Komili, J. West, H. Hieronymus, and P.A. Silver,
1285 *Genome-wide localization of the nuclear transport machinery couples*
1286 *transcriptional status and nuclear organization*. Cell, 2004. **117**(4): p. 427-39.

- 1287 123. Chen, M. and M.R. Gartenberg, *Coordination of tRNA transcription with export at*
1288 *nuclear pore complexes in budding yeast*. Genes Dev, 2014. **28**(9): p. 959-70.
- 1289 124. Gartenberg, M.R. and J.S. Smith, *The Nuts and Bolts of Transcriptionally Silent*
1290 *Chromatin in Saccharomyces cerevisiae*. Genetics, 2016. **203**(4): p. 1563-99.
- 1291 125. Fourel, G., E. Lebrun, and E. Gilson, *Protosilencers as building blocks for*
1292 *heterochromatin*. Bioessays, 2002. **24**(9): p. 828-35.
- 1293 126. Lebrun, E., E. Revardel, C. Boscheron, R. Li, E. Gilson, and G. Fourel,
1294 *Protosilencers in Saccharomyces cerevisiae subtelomeric regions*. Genetics,
1295 2001. **158**(1): p. 167-76.
- 1296 127. Gasser, S.M., F. Hediger, A. Taddei, F.R. Neumann, and M.R. Gartenberg, *The*
1297 *function of telomere clustering in yeast: the circe effect*. Cold Spring Harb Symp
1298 Quant Biol, 2004. **69**: p. 327-37.
- 1299 128. Wang, Y., M. Vujcic, and D. Kowalski, *DNA replication forks pause at silent*
1300 *origins near the HML locus in budding yeast*. Mol Cell Biol, 2001. **21**(15): p.
1301 4938-48.
- 1302 129. Lemoine, F.J., N.P. Degtyareva, K. Lobachev, and T.D. Petes, *Chromosomal*
1303 *translocations in yeast induced by low levels of DNA polymerase a model for*
1304 *chromosome fragile sites*. Cell, 2005. **120**(5): p. 587-98.
- 1305 130. Admire, A., L. Shanks, N. Danzl, M. Wang, U. Weier, W. Stevens, E. Hunt, and
1306 T. Weinert, *Cycles of chromosome instability are associated with a fragile site*
1307 *and are increased by defects in DNA replication and checkpoint controls in yeast*.
1308 Genes Dev, 2006. **20**(2): p. 159-73.
- 1309 131. Kitada, T., T. Schleker, A.S. Sperling, W. Xie, S.M. Gasser, and M. Grunstein,
1310 *gammaH2A is a component of yeast heterochromatin required for telomere*
1311 *elongation*. Cell Cycle, 2011. **10**(2): p. 293-300.
- 1312 132. Keogh, M.C., J.A. Kim, M. Downey, J. Fillingham, D. Chowdhury, J.C. Harrison,
1313 M. Onishi, N. Datta, S. Galicia, A. Emili, J. Lieberman, X. Shen, S. Buratowski,
1314 J.E. Haber, D. Durocher, J.F. Greenblatt, and N.J. Krogan, *A phosphatase*
1315 *complex that dephosphorylates gammaH2AX regulates DNA damage checkpoint*
1316 *recovery*. Nature, 2006. **439**(7075): p. 497-501.
- 1317 133. Cole, H.A., J. Ocampo, J.R. Iben, R.V. Chereji, and D.J. Clark, *Heavy*
1318 *transcription of yeast genes correlates with differential loss of histone H2B*
1319 *relative to H4 and queued RNA polymerases*. Nucleic Acids Res, 2014. **42**(20):
1320 p. 12512-22.
- 1321 134. Ocampo, J., R.V. Chereji, P.R. Eriksson, and D.J. Clark, *The ISW1 and CHD1*
1322 *ATP-dependent chromatin remodelers compete to set nucleosome spacing in*
1323 *vivo*. Nucleic Acids Res, 2016. **44**(10): p. 4625-35.
- 1324 135. Langmead, B. and S.L. Salzberg, *Fast gapped-read alignment with Bowtie 2*. Nat
1325 Methods, 2012. **9**(4): p. 357-9.
- 1326 136. Bray, N.L., H. Pimentel, P. Melsted, and L. Pachter, *Near-optimal probabilistic*
1327 *RNA-seq quantification*. Nat Biotechnol, 2016. **34**(5): p. 525-7.
- 1328 137. Pimentel, H., N.L. Bray, S. Puente, P. Melsted, and L. Pachter, *Differential*
1329 *analysis of RNA-seq incorporating quantification uncertainty*. Nat Methods, 2017.
1330 **14**(7): p. 687-690.

- 1331 138. Hediger, F., F.R. Neumann, G. Van Houwe, K. Dubrana, and S.M. Gasser, *Live*
1332 *Imaging of Telomeres. yKu and Sir Proteins Define Redundant Telomere-*
1333 *Anchoring Pathways in Yeast*. Curr Biol, 2002. **12**(24): p. 2076-89.
1334 139. Heun, P., T. Laroche, K. Shimada, P. Furrer, and S.M. Gasser, *Chromosome*
1335 *dynamics in the yeast interphase nucleus*. Science, 2001. **294**(5549): p. 2181-6.
1336

Figure 1

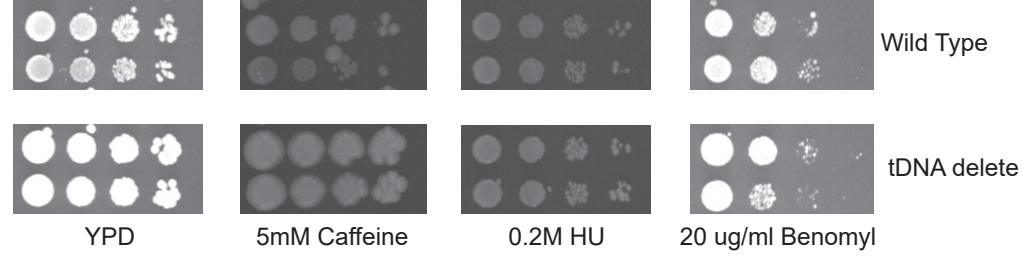


Figure 2

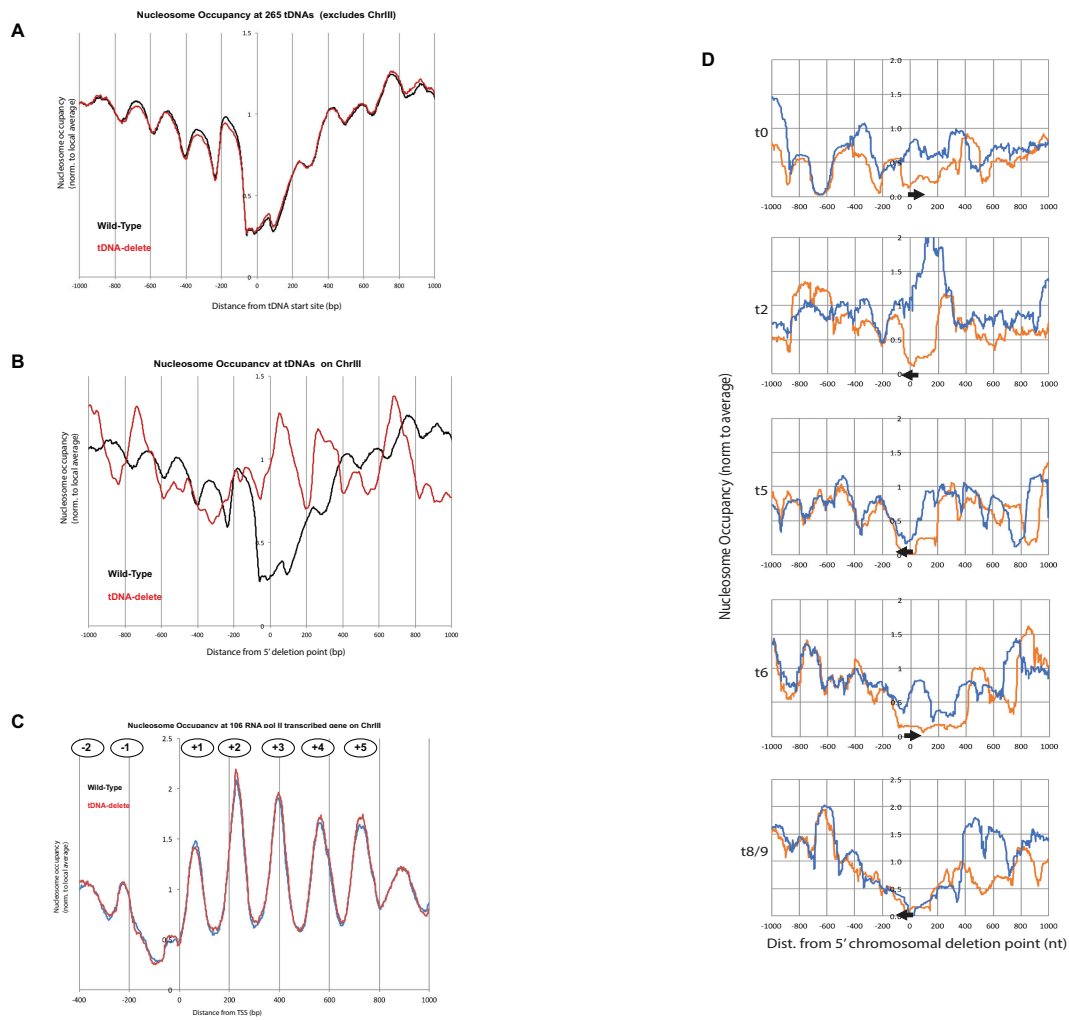
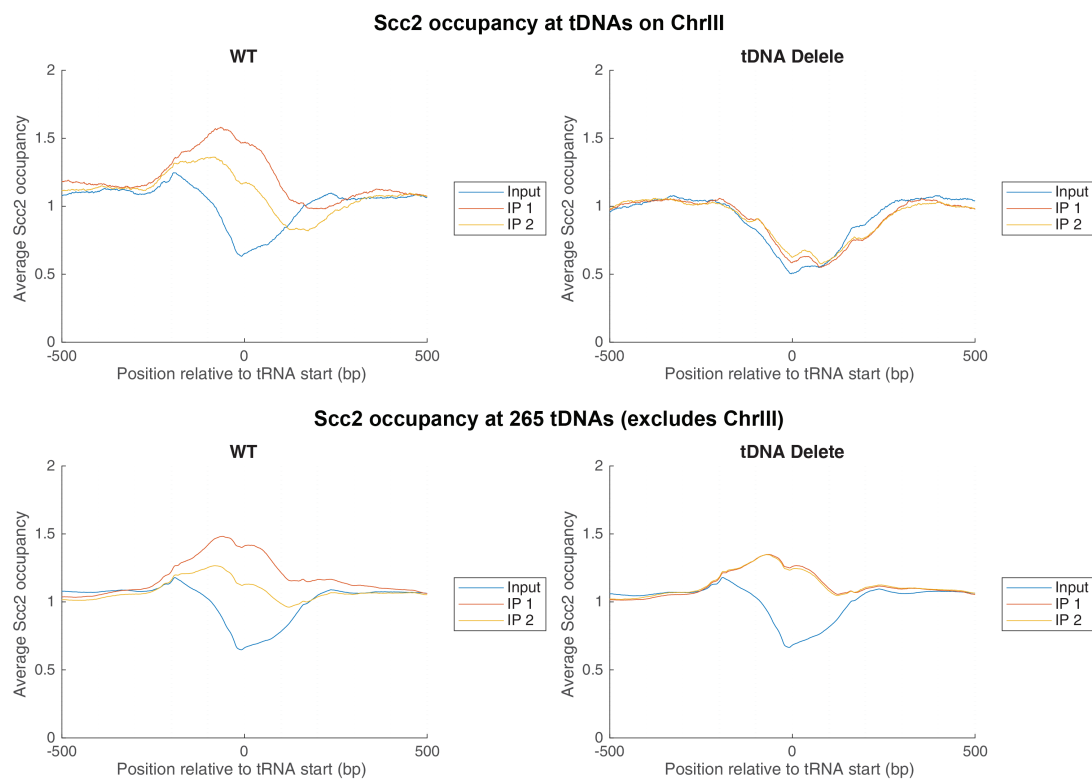


Figure 3



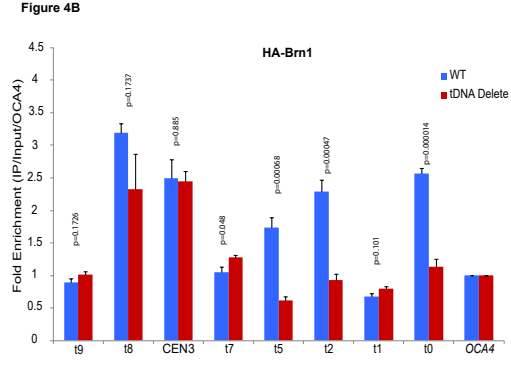
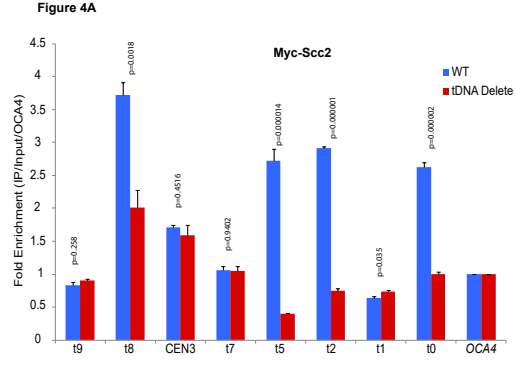


Figure 5

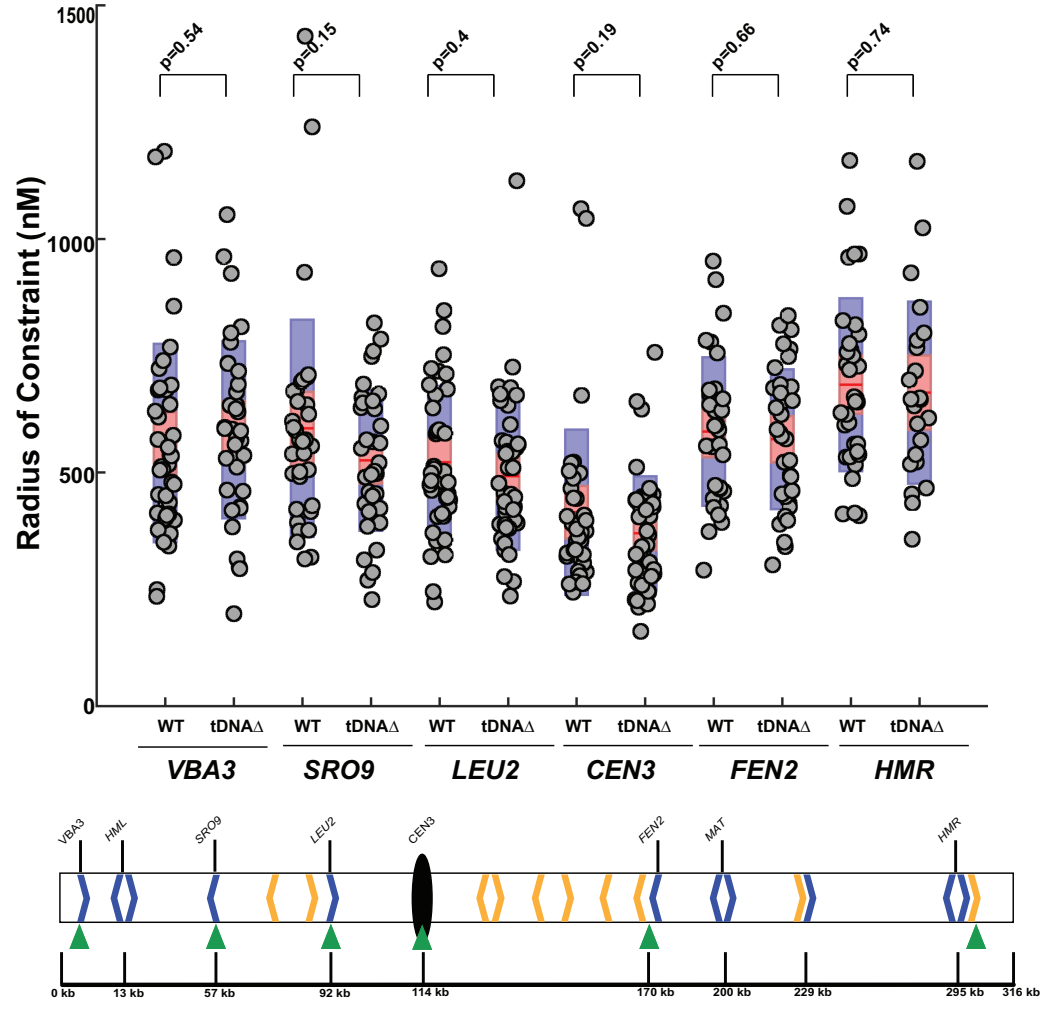


Figure 6

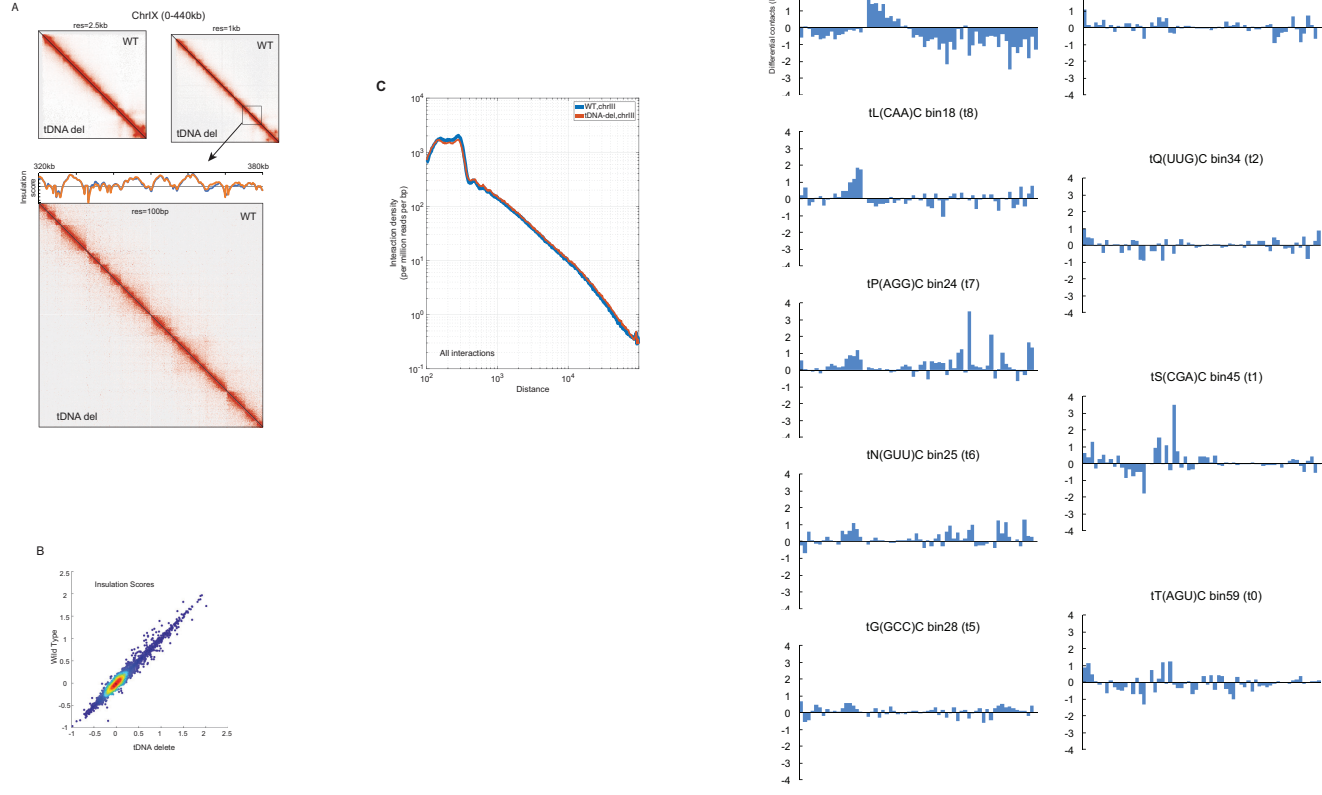


Figure 7

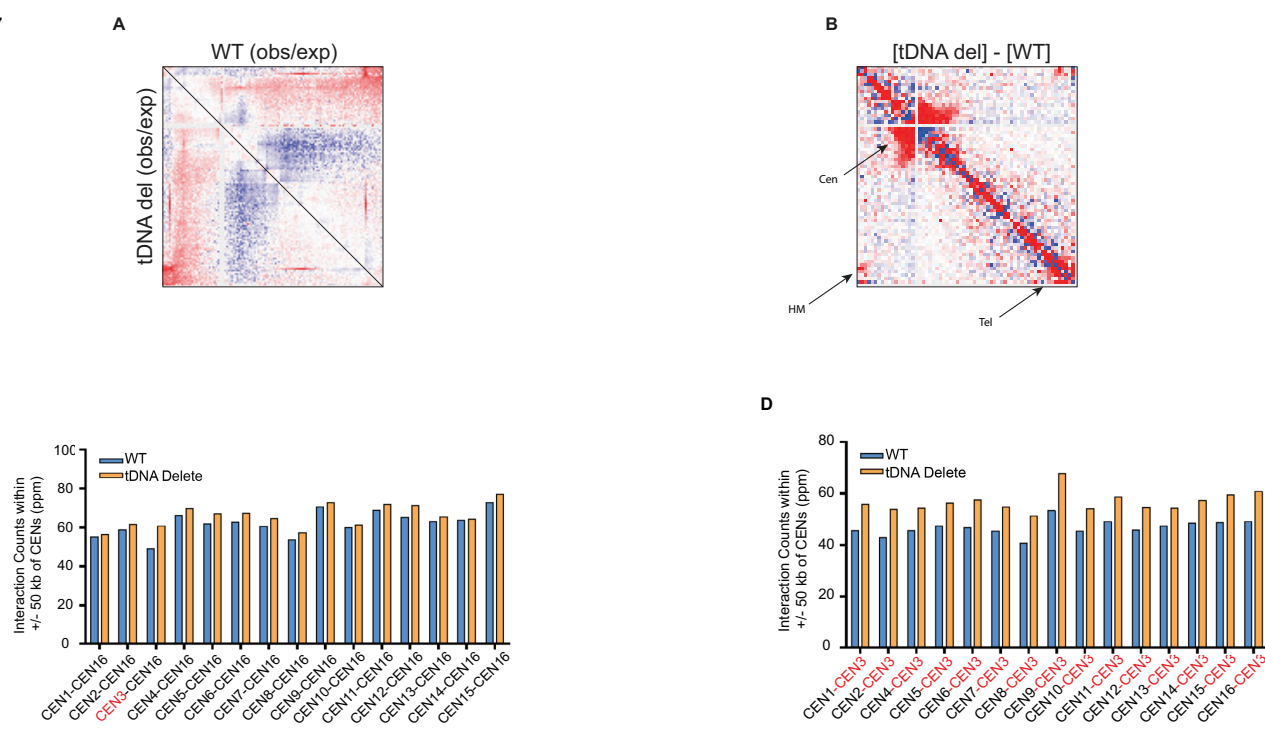


Figure 8A

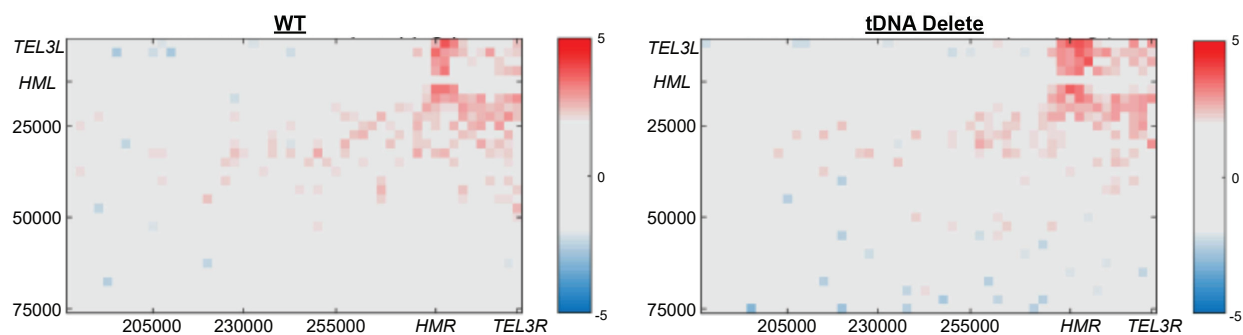


Figure 8B.

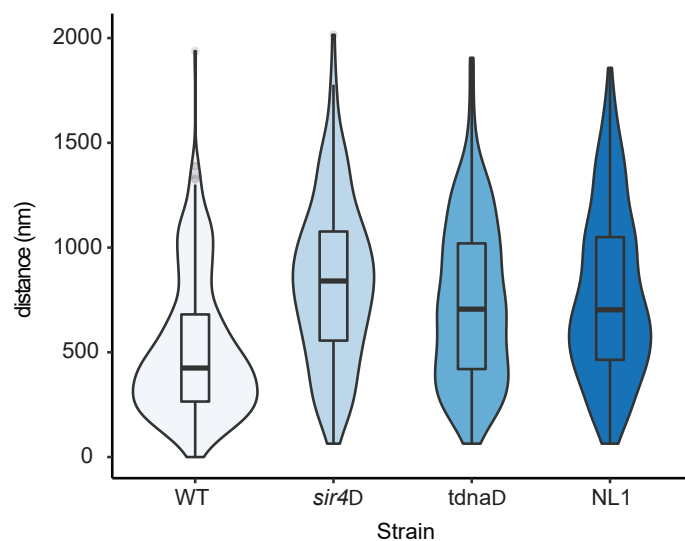


Figure 8C

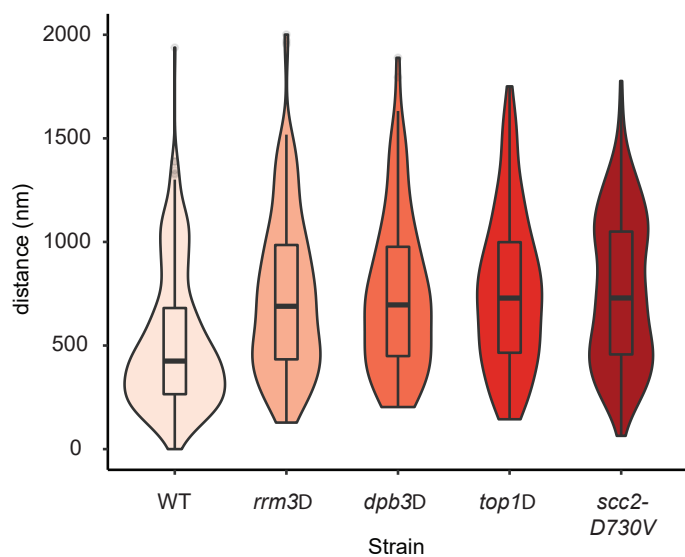


Figure 9A

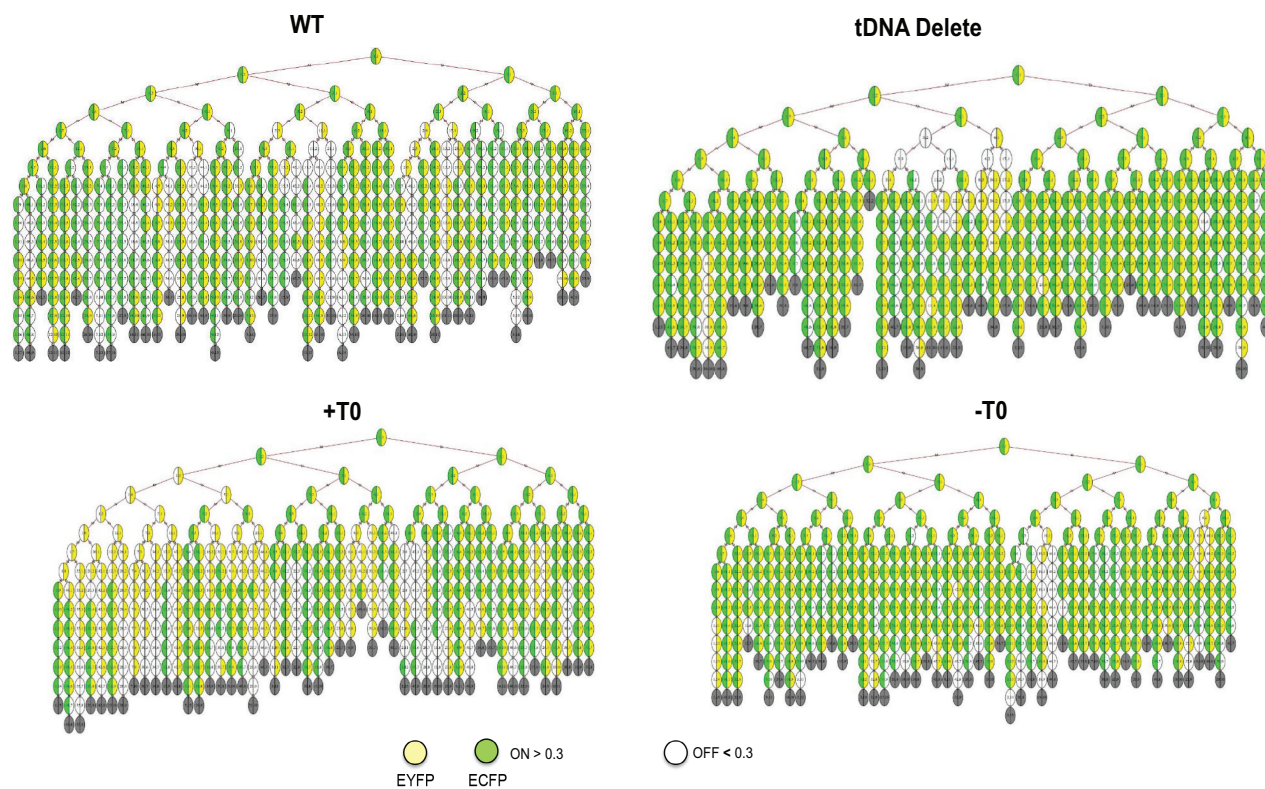
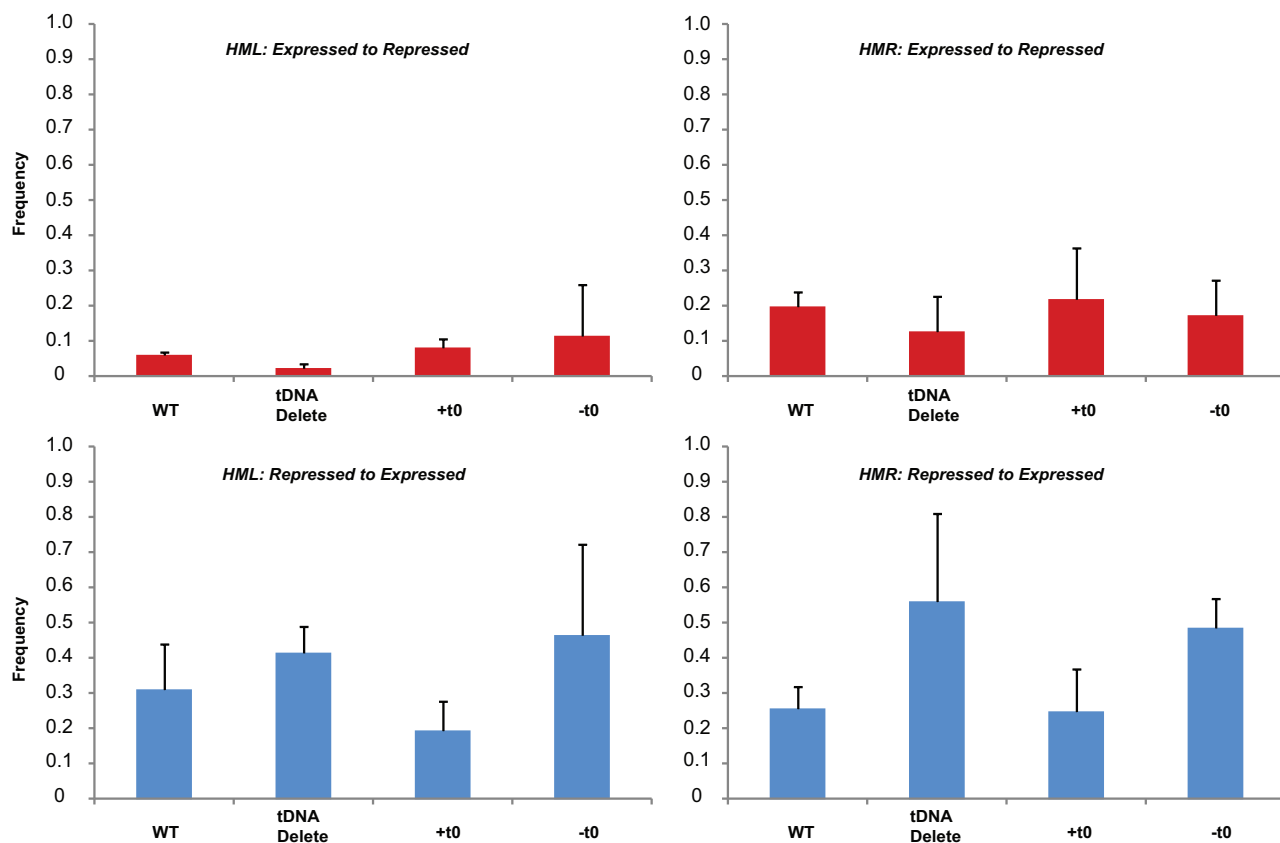


Figure 9B



Upregulated in tDNA del	q-Val (likelihood ratio test)	q val (Wald test)	beta statistic	Gene Name	Function
YCR061w	0.042003857	3.22E-11	0.6580998		Protein of unknown function
YDL124w	0.042003857	6.31E-14	0.4395261		NADPH-dependent alpha-keto amide reductase
YHR214c-B	0.005672182	2.35E-210	2.5870238		Retrotransposon TYA Gag and TYB Pol genes
YNL160w	0.040272092	2.69E-20	0.5348964	YGP1	Cell wall-related secretory glycoprotein
YOR201c	0.020396347	9.18E-27	0.7685378	MRM1	Ribose methyltransferase
YOR202w	0.009117145	1.20E-76	3.7326308	HIS3	Imidazoleglycerol-phosphate dehydratase
YPL240c	0.042003857	1.20E-15	0.5188043	HSP82	Hsp90 chaperone
Downregulated	q-Val (likelihood ratio test)	q val (Wald test)	beta statistic		
YBR068c	0.030966243	1.53E-20	-0.5156825	BAP2	High-affinity leucine permease
YBR296c	0.039894621	1.87E-19	-0.5692597	PHO89	Plasma membrane Na ⁺ /Pi cotransporter
YCR008w	0.015662463	6.48E-43	-1.1217	SAT4	Ser/Thr protein kinase involved in salt tolerance
YER073w	0.045197971	8.81E-16	-0.5691673	ALD5	Mitochondrial aldehyde dehydrogenase
YER091c	0.042003857	1.79E-20	-0.5345605	MET6	Cobalamin-independent methionine synthase
YGL009c	0.009117145	1.47E-82	-2.0202761	LEU1	Isopropylmalate isomerase
YHR208w	0.007776891	7.72E-106	-1.3235331	BAT1	Mitochondrial branched-chain amino acid (BCAA) aminotransferase
YJR010w	0.042003857	3.34E-13	-0.8073784	MET3	ATP sulfurylase involved in methionine metabolism
					Dihydroxyacid dehydratase involved in biosynthesis of branched chain amino acids
YJR016c	0.017736878	3.09E-29	-0.5823368	ILV3	
YKL030w	0.042003857	3.46E-11	-0.6718075		Dubious open reading frame
YKL120w	0.007776891	1.47E-94	-1.4546702	OAC1	Mitochondrial inner membrane transporter
					Acetohydroxyacid reductoisomerase involved in biosynthesis of branched chain amino acids
YLR355c	0.042003857	2.35E-12	-0.387429	ILV5	
YMR108w	0.042003857	3.72E-15	-0.4213145	ILV2	Acetolactate synthase involved in isoleucine and valine biosynthesis
YOR271c	0.027535084	4.63E-26	-0.5903308	FSF1	Putative protein of the sideroblastic-associated protein family

Strain	Genotype Information
JKY562	MATa t0D, t1D, t2D, t3D, t4D, t5D, t6D, t7D, t8D+t9D T1+T7::HIS3 LacI-GFP::ADE2 LEU2 BRN1-HA::KanMx
JKY702	MATa t0D, t1D, t2D, t3D, t4D, t5D, t6D, t7D, t8D+t9D T1+T7::HIS3 Mcd1-13xMyc::KanMx LacI-GFP::ADE2
ROY5151	MATa t0D, t1D, t2D, t3D, t4D, t5D, t6D, t7D, t8D+t9D::LEU2 T1+T7::HIS3 ade2- LYS2+ SCC2-13xMyc::KanMx
ROY4825	MATa HMR(s288c) SCC2-13XMyC::KanMx ADE2 his3 leu2 lys2 trp1 ura3
ROY4925	MATa HMR(s288c) Mcd1-13Xmyc::KanMx ADE2
ROY4927	MATa HMR(s288c) BRN1-HA::KanMx ADE
ROY5750	MATa LacI-GFP::ADE2 lys2- TEL3L::LacO::TRP1 SPC29-RFP::Hyg t0D, t1D, t2D, t3D, t4D, t5D, t6D, t7D, t8D+t9D::LEU2? T1+T7::HIS3
ROY5751	MATa LacI-GFP::ADE2 lys2- TEL3L::LacO::TRP1 SPC29-RFP::Hyg t0D, t1D, t2D, t3D, t4D, t5D, t6D, t7D, t8D+t9D::LEU2? T1+T7::HIS3
ROY5670	LacI-GFP::ADE2 TEL3L::LacO::TRP1 SPC29-RFP::Hyg
ROY5671	LacI-GFP::ADE2 TEL3L::LacO::TRP1 SPC29-RFP::Hyg
ROY5695	LacI-GFP::ADE2 lys2- Chr3L(mid)::LacO::TRP1 SPC29-RFP::Hyg t0D, t1D, t2D, t3D, t4D, t5D, t6D, t7D, t8D+t9D::LEU2 T1+T7::HIS3
ROY5696	LacI-GFP::ADE2 lys2- Chr3L(mid)::LacO::TRP1 SPC29-RFP::Hyg t0D, t1D, t2D, t3D, t4D, t5D, t6D, t7D, t8D+t9D::LEU2 T1+T7::HIS3
ROY5672	LacI-GFP::ADE2 Chr3L(mid)::LacO::TRP1 SPC29-RFP::Hyg
ROY5689	LacI-GFP::ADE2 56xLacO::LEU2 SPC29-RFP::Hyg t0D, t1D, t2D, t3D, t4D, t5D, t6D, t7D, t8D+t9D T1+T7::HIS3
ROY5690	LacI-GFP::ADE2 56xLacO::LEU2 SPC29-RFP::Hyg t0D, t1D, t2D, t3D, t4D, t5D, t6D, t7D, t8D+t9D T1+T7::HIS3
ROY5317	MAT@ LacI-GFP::ADE2 lys- 56xLacO::LEU2 SPC29-RFP::Hyg
ROY5318	MAT@ LacI-GFP::ADE2 lys- 56xLacO::LEU2 SPC29-RFP::Hyg
ROY5290	MAT@ LacI-GFP::ADE2 126xLacO::CEN3::TRP1 spc29-RFP::Hyg t0D, t1D, t2D, t3D, t4D, t5D, t6D, t7D, t8D+t9D T1+T7::HIS3 leu2-
ROY5291	MAT@ LacI-GFP::ADE2 64xLacO::CEN3::TRP1 spc29-RFP::Hyg t0D, t1D, t2D, t3D, t4D, t5D, t6D, t7D, t8D+t9D T1+T7::HIS3 leu2-
ROY5288	MATa LacI-GFP::ADE2 126xLacO::CEN3::TRP1 spc29-RFP::Hyg
ROY5289	MATa LacI-GFP::ADE2 126xLacO::CEN3::TRP1 spc29-RFP::Hyg
ROY5748	MATa LacI-GFP::ADE2 t2::56xLacO::LEU2 SPC29-RFP::Hyg t0D, t1D, t2D, t3D, t4D, t5D, t6D, t7D, t8D+t9D T1+T7::HIS3 leu2-
ROY5749	MATa LacI-GFP::ADE2 t2::56xLacO::LEU2 SPC29-RFP::Hyg t0D, t1D, t2D, t3D, t4D, t5D, t6D, t7D, t8D+t9D T1+T7::HIS3 leu2-
ROY5668	MAT@ LacI-GFP::ADE2 t2wt::56xLacO::LEU2 SPC29-RFP::Hyg
ROY5669	MAT@ LacI-GFP::ADE2 t2wt::56xLacO::LEU2 SPC29-RFP::Hyg
ROY5319	MATa LacI-GFP::ADE2 lys- MAT::LacO::TRP1 SPC29-RFP::Hyg t0D, t1D, t2D, t3D, t4D, t5D, t6D, t7D, t8D+t9D::LEU2 T1+T7::HIS3
ROY5320	MATa LacI-GFP::ADE2 lys- MAT::LacO::TRP1 SPC29-RFP::Hyg t0D, t1D, t2D, t3D, t4D, t5D, t6D, t7D, t8D+t9D::LEU2 T1+T7::HIS3
ROY5294	MAT@ LacI-GFP::ADE2 MAT::LacO::TRP1 lys- SPC29-RFP::Hyg
ROY5359	MAT@ LacI-GFP::ADE2 lys- MAT::LacO::TRP1 SPC29-RFP::Hyg
ROY5687	MATa LacI-GFP::ADE2 t1::56xLacO::LEU2 SPC29-RFP::Hyg t0D, t1D, t2D, t3D, t4D, t5D, t6D, t7D, t8D+t9D T1+T7::HIS3 leu2-
ROY5688	MAT@ LacI-GFP::ADE2 t1::56xLacO::LEU2 SPC29-RFP::Hyg t0D, t1D, t2D, t3D, t4D, t5D, t6D, t7D, t8D+t9D T1+T7::HIS3 leu2-
ROY5666	MAT@ LacI-GFP::ADE2 t1wt::56xLacO::LEU2 SPC29-RFP::Hyg
ROY5667	MAT@ LacI-GFP::ADE2 t1wt::56xLacO::LEU2 SPC29-RFP::Hyg
ROY5321	MAT@ LacI-GFP::ADE2 lys- GIT1::56xLacO::TRP1 SPC29-RFP::Hyg t0D, t1D, t2D, t3D, t4D, t5D, t6D, t7D, t8D+t9D::LEU2 T1+T7::HIS3
ROY5323	MAT@ LacI-GFP::ADE2 lys- GIT1::56xLacO::TRP1 SPC29-RFP::Hyg t0D, t1D, t2D, t3D, t4D, t5D, t6D, t7D, t8D+t9D::LEU2 T1+T7::HIS3
ROY5664	LacI-GFP::ADE2 GIT1::56xLacO::TRP1 SPC29-RFP::Hyg
ROY5665	LacI-GFP::ADE2 GIT1::56xLacO::TRP1 SPC29-RFP::Hyg
JKY689	MATa tDNA0 (WT) t1D, t2D, t3D, t4D, t5D, t6D, t7D, t8D+t9D T1+T7::HIS3 LEU2 ade2-1
ROY1681	MAT@ ADE2 his3 leu2 lys2 trp1 ura3 HMR (t-RNA bound delete)
JKY690	MATa t0D, t1D, t2D, t3D, t4D, t5D, t6D, t7D, t8D+t9D T1+T7::HIS3 LEU2 ade2-1 LYS+
JRY2334	MATa ade2-1 can1-100 his3-11 leu2-3,112 trp1-1 ura3-1 GAL
ROY4830	MATa/MAT@ HML-TetO :: LEU2 HMR-LacO:: TRP1 CFP-LacI-TetR-YFP::ADE2 LYS2
ROY4846	MAT@ LacO(256x)::GIT1::TRP1 HML-TetO::LEU2 CFP-LacI-TetR-YFP::ADE2 tT(AGU)CA::URA3 lys2Δ
ROY4859	MAT HML-tetO::LEU2 HMR-LacO::TRP1 CFP-LacI-TetR-YFP::ADE2 sir4Δ::URA3 lys-

ROY4860	MAT HML-tetO::LEU2 HMR-LacO::TRP1 CFP-LacI-TetR-YFP::ADE2 sir4Δ::URA3 lys-
ROY5518	MATa LacI-GFP::ADE2 lys2- Chr3L(mid)::LacO::TRP1 t0D, t1D, t2D, t3D, t4D, t5D, t6D, t7D, t8D+t9D::LEU2 T1+T7::HIS3
ROY5521	MATa lys- LacI-GFP::ADE2 Chr3L(mid)::LacO::TRP1
ROY5602	MATa LacI-GFP::ADE2 56xLacO::LEU2 t0D, t1D, t2D, t3D, t4D, t5D, t6D, t7D, t8D+t9D T1+T7::HIS3
GRY911	MATa LacI-GFP::ADE2 56xLacO::LEU2 lys-
GRY907	MAT@ LacI-GFP::ADE2 56xLacO::LEU2 lys- trp- ura- his-
GRY872	MAT@ 126xLacO::CEN3::TRP1 t0D, t1D, t2D, t3D, t4D, t5D, t6D, t7D, t8D+t9D T1+T7::HIS3 leu2-3, 112 LacI-GFP::ADE2 trp- lys- ura-
GRY823	Mata LacI-GFP::ADE2 LacO(64x)::CEN3::TRP1
GRY824	MAT@ LacI-GFP::ADE2 LacO(64x)::CEN3::TRP1
ROY5512	MATa LacI-GFP::ADE2 t2::56xLacO::LEU2 t0D, t1D, t2D, t3D, t4D, t5D, t6D, t7D, t8D+t9D T1+T7::HIS3 leu2-
ROY5510	MAT@ lys- LacI-GFP::ADE2 t2wt::56xLacO::LEU2
GRY938	MAT@ t1Δ::URA3 t0D, t1D, t2D, t3D, t4D, t5D, t6D, t7D, t8D+t9D::LEU2 T1+T7::HIS3 LacI-GFP::ADE2 HMR-GIT1::TRP1 lys-
GRY883	MAT@ t1WT@HIS3 t1WT::URA3 GIT1::TRP1 LYS+ LEU+ ade-
GRY935	MATa LacI-GFP::ADE2 t0D, t1D, t2D, t3D, t4D, t5D, t6D, t7D, t8D+t9D T1+T7::HIS3 trp- leu- lys- ura-
GRY963	MAT@ t0D, t1D, t2D, t3D, t4D, t5D, t6D, t7D, t8D+t9D T1+T7::HIS3 LYS+ ade- leu-
JRY4012	MATa can1-100 his3-11 leu2-3,112 lys2Δ trp1-1 ura3-1 GAL

Primer Name	Sequence 5'-3'	Amplicon
yOH58	TACTACAAGAGAAAAGGCCATCTCC	t1
yOH59	AATGCAGCGCAGACAGCACAGTT	t1
QJK61	TTGAGATACAAAATATTACAAGAAGTCCTG	t2
QJK62	GCGTTCTTCTGTATCTGAAGATAGTG	t2
QJK63	TCATGTATCAAGATTACTAGCGCAAGTG	t5
QJK64	TTCTATTCTTATGTACCGTTCCGCC	t5
yOH62	GCAAGCGAAGTTGTTCCCGTTAT	t7
yOH63	GTTCCGGTCACTTAGAGGATATAATTG	t7
QJK69	CTCTATTTCTCAACAAGTAATTGGTTGTTT	t8
QJK70	GCCCCTGTGTGTTCTCGTTATGT	t8
yOH64	GACAAGAAAAGATAACGACACAGTGA	t9
yOH65	GGCCCTCGTATAGTCTCTTTTC	t9
R197	GAGACCAGGTTTATTCAACCGGTAAC	t0
LOU120	GGGTGTCACCGAATAACGTGAT	t0
GRO39	TAAGACAATTGTGGACAACAAAGCAAA	OCA4
GRO40	ATTTATTAATGTCAAAAGCCGCTGAGG	OCA4
yOH66	TCACTCATATAAACCGAACCCTTCC	CEN3
yOH67	GGATTTTCCATATTGTTTGCGCTG	CEN3

	HMR (Exp to Rep)	HMR (Rep to Exp)	HML (Exp to Rep)	HML (Rep to Exp)
WT	0.2 (0.019)	0.25 (0.031)	0.06 (0.005)	0.3 (0.075)
tDNA Delete	0.13 (0.057)	0.56 (0.145)	0.02 (0.006)	0.41 (0.041)
t0+	0.22 (0.085)	0.25 (0.070)	0.08 (0.014)	0.19 (0.049)
t0-	0.18 (0.049)	(0.48 (0.041)	0.11 (0.072)	0.46 (0.12)